Exogenous TNFR2 activation protects from acute GvHD via host T reg cell expansion

Martin Chopra,[1,3] Marlene Biehl,[1,3] Tim Steinfatt,[1,3,4] Andreas Brandl,[1,3] Juliane Kums,[2] Jorge Amich,[1,3] Martin Vaeth,[6] Janina Kuen,[6] Rafaela Holtappels,[9] Jürgen Podlech,[9] Anja Mottok,[5] Sabrina Kraus,[1,3] Ana-Laura Jordán-Garrote,[1,3,4] Carina A. Bäuerlein,[1,3,4] Christian Brede,[1,3,4] Eliana Ribechini,[8] Andrea Fick,[2] Axel Seher,[2] Johannes Polz,[10] Katja J. Ottmüller,[1,3,4] Jeanette Baker,[11] Hidekazu Nishikii,[11] Miriam Ritz,[1,3] Katharina Mattenheimer,[1,3] Stefanie Schwinn,[1,3] Thorsten Winter,[1,3] Viktoria Schäfer,[2] Sven Krappmann,[12] Hermann Einsele,[1] Thomas D. Müller,[7] Matthias J. Reddehase,[9] Manfred B. Lutz,[8] Daniela N. Männel,[10] Friederike Berberich-Siebelt,[6] Harald Wajant,[2]* and Andreas Beilhack[1,3,4]*

[1]Department of Internal Medicine II, University Hospital Würzburg, [2]Division of Molecular Internal Medicine, Department of Internal Medicine II, University Hospital Würzburg, [3]Center for Interdisciplinary Clinical Research, [4]Graduate School of Life Sciences, [5]Institute of Pathology, [6]Department of Molecular Pathology, Institute of Pathology, [7]Department for Molecular Plant Physiology and Biophysics, Julius-von-Sachs Institute, and [8]Institute for Virology and Immunobiology, Würzburg University, 97080 Würzburg, Germany
[9]Institute for Virology and Research Center of Immunotherapy, University Medical Center of the Johannes Gutenberg-University, 55131 Mainz, Germany
[10]Institute of Immunology, Regensburg University, 93053 Regensburg, Germany
[11]Blood and Marrow Transplantation, Stanford University School of Medicine, Stanford, CA 94305
[12]Microbiology Institute, Clinical Microbiology, Immunology and Hygiene, University Hospital Erlangen and Friedrich-Alexander University Erlangen-Nürnberg, 91054 Erlangen, Germany

Donor CD4$^+$Foxp3$^+$ regulatory T cells (T reg cells) suppress graft-versus-host disease (GvHD) after allogeneic hematopoietic stem cell transplantation (HCT [allo-HCT]). Current clinical study protocols rely on the ex vivo expansion of donor T reg cells and their infusion in high numbers. In this study, we present a novel strategy for inhibiting GvHD that is based on the in vivo expansion of recipient T reg cells before allo-HCT, exploiting the crucial role of tumor necrosis factor receptor 2 (TNFR2) in T reg cell biology. Expanding radiation-resistant host T reg cells in recipient mice using a mouse TNFR2-selective agonist before allo-HCT significantly prolonged survival and reduced GvHD severity in a TNFR2- and T reg cell–dependent manner. The beneficial effects of transplanted T cells against leukemia cells and infectious pathogens remained unaffected. A corresponding human TNFR2-specific agonist expanded human T reg cells in vitro. These observations indicate the potential of our strategy to protect allo-HCT patients from acute GvHD by expanding T reg cells via selective TNFR2 activation in vivo.

INTRODUCTION

Allogeneic hematopoietic stem cell transplantation (HCT [allo-HCT]) is the only curative treatment for several malignant and nonmalignant hematopoietic diseases. Alloreactive T cells mediate the beneficial graft-versus-leukemia/lymphoma (GvL) effect and detrimental graft-versus-host disease (GvHD), the main reason for nonrelapse mortality after allo-HCT (Welniak et al., 2007; Li and Sykes, 2012). Donor-derived CD4$^+$Foxp3$^+$ regulatory T cells (T reg cells) suppress GvHD in preclinical mouse models of allo-HCT, while maintaining the antitumoral effects of transplanted conventional T cells (T con cells; Hoffmann et al., 2002; Edinger et al., 2003; Trenado et al., 2003; Nguyen et al., 2007; Pierini et al., 2015). Co-infusion of human T con cells and T reg cells into immunodeficient mice bearing HLA-mismatched human leukemia cells resulted in the rejection of the leukemia without the development of GvHD (Martelli et al., 2014). The positive effects of the use of donor T reg cells in the treatment or prophylaxis of GvHD are mirrored in clinical studies in which the occurrence of both GvHD and tumor relapse were markedly reduced. Nevertheless, the use

*H. Wajant and A. Beilhack contributed equally to this paper.

Correspondence to Andreas Beilhack: beilhack_a@ukw.de; or Harald Wajant: harald.wajant@mail.uni-wuerzburg.de

M. Chopra's present address is Dept. of Molecular Medicine and Pathology, Faculty of Medical and Health Sciences, University of Auckland, Auckland 1023, New Zealand.

M. Vaeth's present address is Dept. of Pathology and Cancer Institute, New York University School of Medicine, New York, NY 10016.

A. Mottok's present address is Dept. of Lymphoid Cancer Research, BC Cancer Agency, Vancouver, British Columbia V5Z 1L3, Canada.

A. Seher's present address is Dept. of Oral and Maxillofacial Plastic Surgery, University Hospital Würzburg, Würzburg University, 97080 Würzburg, Germany.

Abbreviations used: ALP, alkaline phosphatase; BLI, bioluminescence imaging; bw, body weight; DTx, diphtheria toxin; eGFP, enhanced GFP; GpL, *Gaussia princeps* luciferase; GvHD, graft-versus-host disease; GvL, graft versus leukemia/lymphoma; HCT, hematopoietic stem cell transplantation; ICOS, inducible T cell co-stimulator; mCMV, mouse CMV; MDSC, myeloid-derived suppressor cell; TNC, tenascin C.

The Rockefeller University Press $30.00
J. Exp. Med. 2016 Vol. 213 No. 9 1881–1900
www.jem.org/cgi/doi/10.1084/jem.20151563

of donor T reg cells is challenging with regard to the numbers and purity of the required cells as well as to their stability after infusion into allo-HCT recipients. Current study protocols are based on the ex vivo expansion of these cells and/or their infusion in high numbers (Brunstein et al., 2011; Di Ianni et al., 2011; Edinger and Hoffmann, 2011; Veerapathran et al., 2013; Martelli et al., 2014).

TNF and its receptors TNFR1 and TNFR2 play a crucial role in both GvHD and the GvL reaction (Levine, 2011). TNF, through the activation of TNFR1, causes inflammation and tissue damage (Feldmann and Maini, 2003; Chopra et al., 2015), whereas the activation of TNFR2 exerts immunesuppressive functions (Robinson et al., 2001; Ramos-Casals et al., 2008; Ko et al., 2009). TNF affects both mouse and human T reg cells, with TNFR2 being a decisive factor (Valencia et al., 2006; Chen et al., 2007, 2008; Lin et al., 2008; Grinberg-Bleyer et al., 2010; Nagar et al., 2010; Nie et al., 2013; Okubo et al., 2013). The TNF–TNFR2 interaction is crucial for T reg cell–mediated effects in various mouse models, including autoimmune-mediated colitis (Housley et al., 2011; Chen et al., 2013), experimental autoimmune encephalomyelitis (Tsakiri et al., 2012), and the growth of B16F10 mouse melanoma pulmonary metastases (Chopra et al., 2013a).

We developed a novel protein agonist (selective mouse TNF-based agonist of TNF receptor 2 [STAR2]) that selectively activates mouse TNFR2 and expands and activates natural T reg cells (nT reg cells) in vitro and in vivo. The human TNF-based counterpart of this agonist expanded human T reg cells in vitro. Treatment of recipient mice with STAR2 before allo-HCT expanded host-type radiation-resistant T reg cells and resulted in a significantly improved outcome after allo-HCT and prolonged survival without inhibiting the antileukemia or antiinfective effects of transplanted T con cells.

RESULTS

STAR2 is a highly active mouse TNF-based agonist of TNFR2 devoid of TNFR1 stimulatory activity

TNFR2 is highly expressed on T reg cells, and its activation has been associated with the expansion and enhanced function of this cell type (Chen et al., 2007; Housley et al., 2011; Chopra et al., 2013a; Okubo et al., 2013). We were therefore interested in experimentally evaluating in preclinical in vivo models of allo-HCT the idea that TNFR2 targeting induces T reg cell expansion and protection from GvHD. Both soluble and membrane-bound TNF can bind to TNFR2, but only the membrane-bound form efficiently activates TNFR2 (Grell et al., 1995). It has, however, been demonstrated that oligomerized soluble TNF molecules acquire a high membrane TNF-like TNFR2 stimulatory activity (Schneider et al., 1998; Rauert et al., 2010). As the available human TNF-based TNFR2-specific TNF muteins cannot be used in mice because of the species specificity of the TNF–TNFR2 interaction, we constructed a nonameric TNFR2-specific variant of mouse TNF (STAR2) by fusing a single-chain mouse TNF trimer to the trimerization domain of chicken tenascin C (TNC; Fig. 1 A). TNFR2 specificity was accomplished by a steric clash between STAR2 and mouse TNFR1 as the result of two amino acid exchanges (D221N and A223R) within the individual TNF subunits (Fig. 1 B). The introduction of the TNC trimerization domain into the STAR2 molecule causes spontaneous oligomer formation to mimic membrane-bound TNF (Fig. 1 C).

Both wild-type mouse TNF and STAR2 were able to bind to mouse TNFR2 (Fig. 1 D), whereas only the wild-type form but not STAR2 also interacted with TNFR1 (Fig. 1 E). Human TNF, which only activates mouse TNFR1 but not TNFR2 (Lewis et al., 1991), inhibited the bone morphogenetic protein 2 (BMP2)–induced production of alkaline phosphatase (ALP) in mouse preosteoblastic C2C12 cells, whereas STAR2 failed to do so (Fig. 1 F). A nonameric wild-type variant of mouse TNF, but not STAR2, reduced the viability of mouse L929 cells, which are highly sensitive to TNFR1-induced cell death (Fig. 1 G). However, STAR2 efficiently killed cells from a TNFR1/2-deficient immortalized embryonic mouse fibroblast line that was reconstituted with a chimeric receptor, in which the extracellular domain of the death receptor CD95 was replaced by mouse TNFR2 (Fig. 1 H). Altogether, these in vitro studies confirmed the TNFR2-specific activity of STAR2 expected based on the initial binding studies.

STAR2 expands and activates T reg cells in mixed T cell cultures in vitro

We isolated splenic T cells from healthy young adult mice and incubated them with STAR2 in the absence of any other T cell stimulatory factors. Selective TNFR2 activation with STAR2 expanded $CD4^+Foxp3^+$ T reg cells from wild-type but not TNFR2-deficient mice (Fig. 2, A and B). This was observed in both $CD4^+/CD8^+$ T cell cultures (Fig. 2, A and B) and in purified $CD4^+$ T cell cultures of different mouse strains (Fig. 2 C). The increase in relative numbers of T reg cells in the cultures was accompanied by increased proliferation of these cells but not of T con cells, as demonstrated by CFSE dilution. T reg cells deficient for TNFR2 did not proliferate in response to STAR2 treatment (Fig. 2 D). We observed a preferential up-regulation of activation markers CD103, inducible T cell co-stimulator (ICOS), CD69, and CD44 on T reg cells upon STAR2 treatment. ICAM-1 was induced on both T reg cells and T con cells, but on the latter cells to a far lesser degree. CD44 on T con cells was down-regulated by STAR2 (Fig. 2 E).

To evaluate the relevance of IL-2 for TNFR2-mediated T reg cell expansion, we treated isolated $CD4^+$ T cells with STAR2, IL-2, rapamycin, and various combinations of these reagents. STAR2 and IL-2 expanded T reg cells to a similar extent and showed no additive effect. Rapamycin enhanced IL-2–induced T reg cell expansion but showed no effect on STAR2-induced T reg cell expansion (Fig. 2 F). Treating T cells with STAR2 in the presence of IL-2–blocking antibodies ablated the T reg cell–expanding effect of TNFR2 ac-

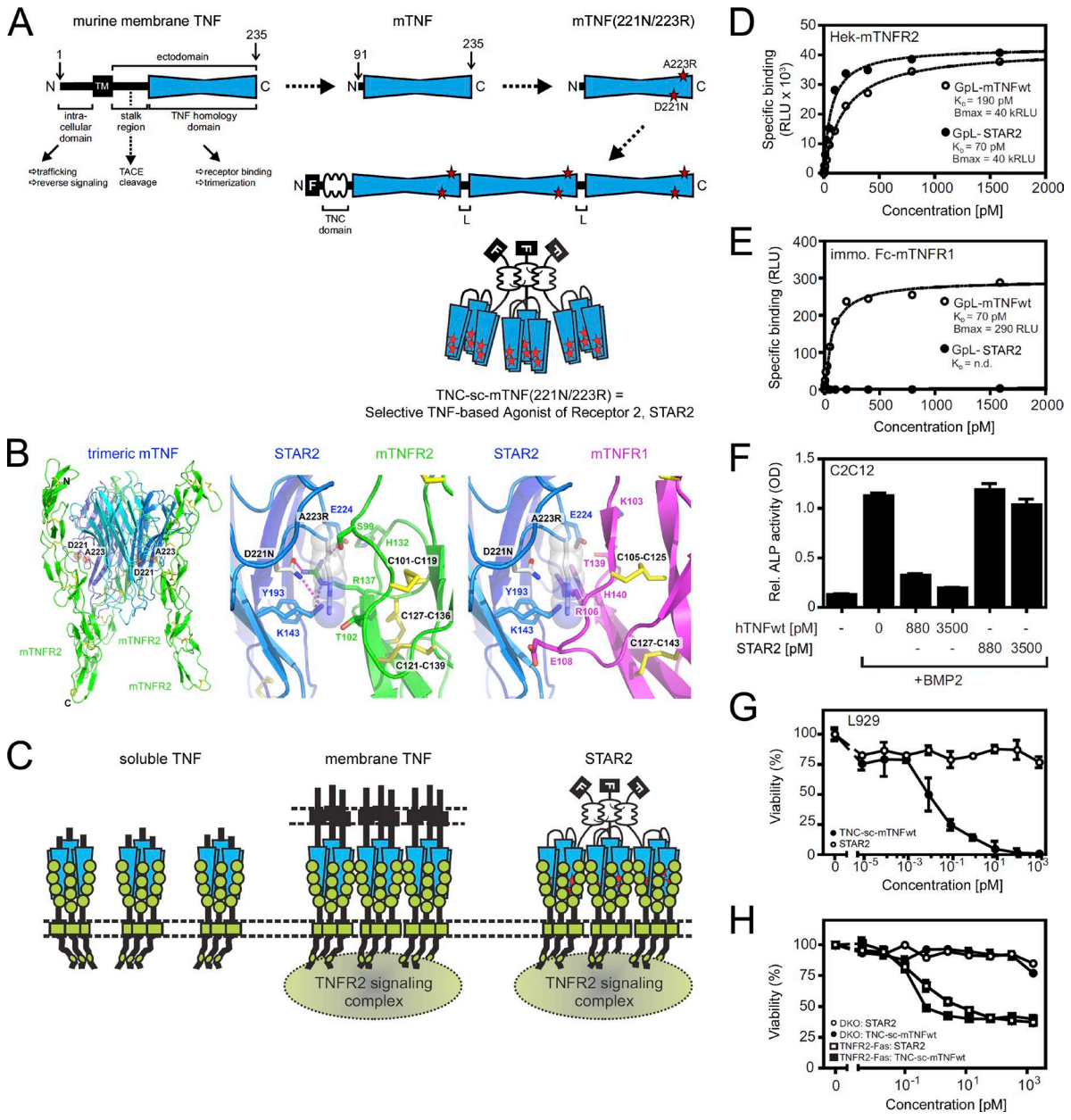

Figure 1. **STAR2 is a selective agonist for TNFR2.** (A) Three linker-connected mouse TNF(D221N-A223R) protomers were fused to the trimerization domain of chicken TNC, resulting in the formation of the STAR2 molecule with three covalently linked TNF trimers. F, Flag tag; L, linker; TACE, TNF-α converting enzyme; TM, transmembrane domain. (B) Homology model of the extracellular part of mouse TNF (mTNF) bound to the ectodomain of mouse TNFR2 (overview; left). The arginine side chain introduced at position 223 of STAR2 fits into mouse TNFR2 (middle) but leads to a steric clash with mouse TNFR1 (right). (C) Soluble trimeric TNF binds to but does not properly activate TNFR2, whereas membrane-bound TNF binds to and activates TNFR2. Both soluble and membrane-bound TNF bind and activate TNFR1 (not depicted). Nonameric STAR2 binds to and activates only TNFR2 because of mutations preventing TNFR1 binding. (D) Binding assay for mouse TNFR2. Hek293 cells were transiently transfected with mouse TNFR2 and incubated with a GpL fusion protein of mouse TNF and STAR2. (E) Binding assay for mouse TNFR1. Immobilized (immo.) Fc–mouse TNFR1, an Fc fusion protein containing the ectodomain of mouse TNFR1, was incubated with GpL–mouse TNF and GpL-STAR2. n.d., not determined. (D and E) Representative data are from two independent experiments. RLU, relative light units. (F) Mouse preosteoblastic C2C12 cells were treated with BMP2 in the presence and absence of STAR2 and human TNF (hTNF) before the BMP2-induced production of ALP was determined. Rel., relative. (G) Mouse L929 cells were challenged with nonameric wild-type TNF and STAR2. Viability was determined by crystal violet staining. (H) Immortalized mouse TNFR1–TNFR2 double KO (DKO) embryonic fibroblasts expressing a chimeric receptor of the mouse TNFR2 ectodomain and the intracellular part of human CD95 were stimulated in 96-well plates in triplicates with nonameric wild-type TNF and STAR2. Viability was determined by crystal violet staining. (F–H) Data are mean ± SEM of triplicates and are representative of two independent experiments.

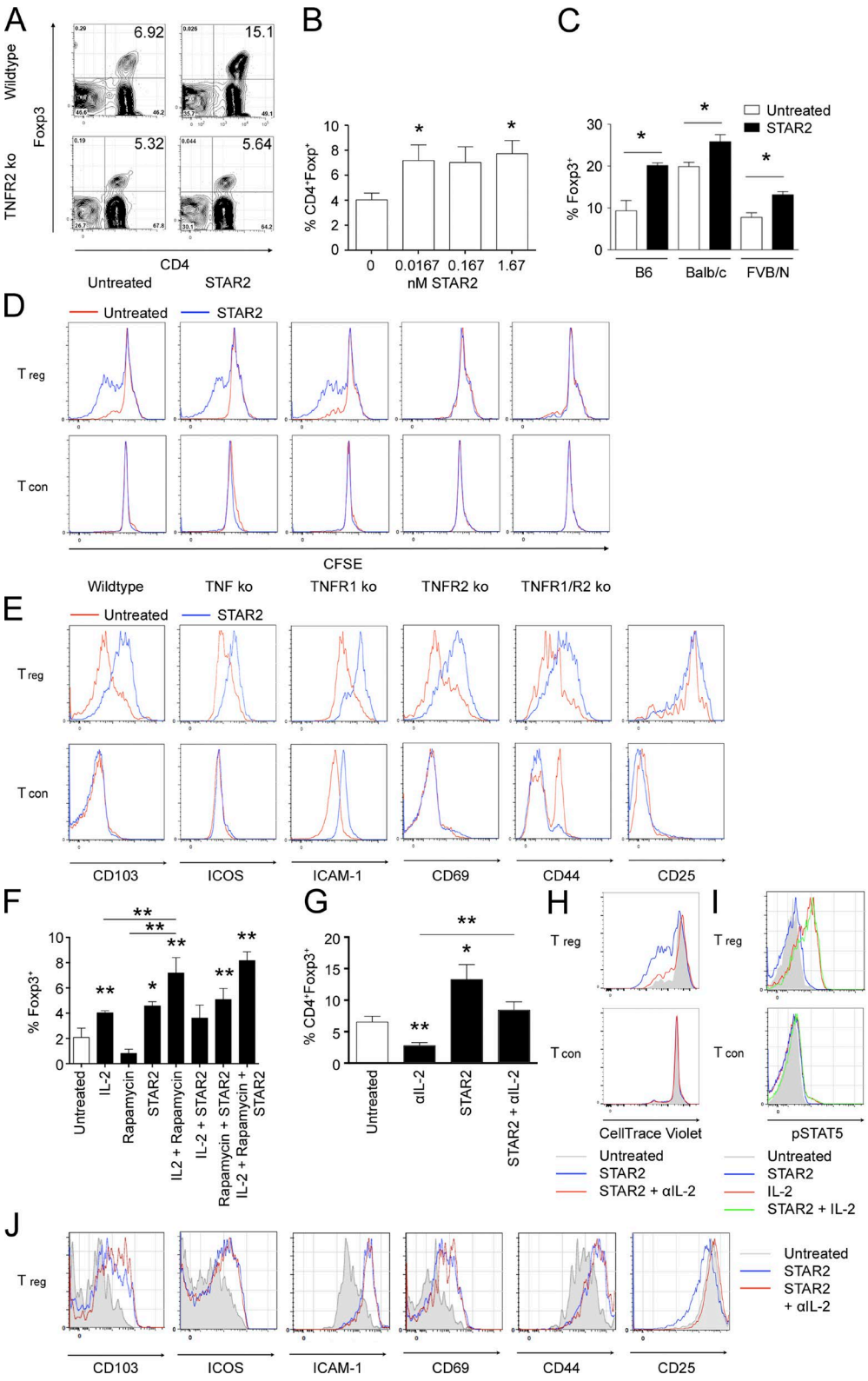

Figure 2. **STAR2 expands and activates T reg cells in vitro.** (A) Wild-type or TNFR2 KO B6 $CD4^+/CD8^+$ T cells were treated with 1.67 nM STAR2 for 96 h and analyzed for CD4 and Foxp3 expression. Representative data are from five independent experiments. (B) B6.Foxp3.Luci.DTR-4 $CD4^+/CD8^+$ T cells were treated with STAR2 for 96 h and analyzed for CD4 and Foxp3-eGFP expression. Combined data are from six independent experiments. (C) CD4 T cells were purified from spleens of B6 ($n = 6$), BALB/c ($n = 6$), and FVB/N ($n = 3$) mice and treated with STAR2 for 96 h. The frequency of T reg cells among CD4 T cells

tivation. Importantly, blocking IL-2 in the absence of STAR2 also significantly reduced T reg cell percentages in the cultures, and STAR2 significantly increased these numbers (Fig. 2, G and H). Interestingly, treatment of mixed $CD4^+$ T con cell/T reg cell cultures with IL-2 but not STAR2 increased STAT5 phosphorylation in T reg cells but not in T con cells (Fig. 2 I). Blocking IL-2 did not affect the induction of activation markers on T reg cells by STAR2 (Fig. 2 J) despite the strong inhibiting effect of IL-2 blockade on T reg cell expansion and proliferation.

A recent study has demonstrated that TNFR2 activation results in IL-2 expression in $CD4^+$ T cells (Miller et al., 2015), and our results indicate that IL-2 may be required for some but not all of the effects of STAR2 observed on T reg cells in vitro. Future studies must show whether T reg cell expansion by STAR2 is merely dependent on the presence of constitutively produced IL-2 present in the T cell culture models used here or whether it actively triggers IL-2 production in T reg cells and/or T con cells. The latter are only poorly engaged by STAR2, but this does not necessarily rule out a contribution of this subset to IL-2 production.

STAR2 expands purified T reg cells but neither modifies T reg cell suppressive activity on a per cell basis nor induces the conversion of T reg cells from T con cells

We next assessed the effects of STAR2 on purified T reg cells in the absence of other cells. TNFR2 activation in purified T reg cell cultures induced proliferation as demonstrated by [^{3}H]thymidine incorporation (Fig. 3 A) and expanded these cells independently of the availability of IL-2 (Fig. 3 B). STAR2 induced the expression of CD103, ICAM-1, and CD69 on purified T reg cells but not of ICOS or CD44 (Fig. 3 C), in contrast to its effect in mixed T cell cultures (Fig. 2 E). Blocking IL-2 did not affect activation marker expression in T reg cell cultures, consistent with the results observed in mixed cultures (Fig. 2 J).

Despite inducing T reg cell proliferation in mixed T cell cultures, STAR2 did not significantly modulate Foxp3 expression in treated T reg cells in such cultures when compared with untreated cells (Fig. 3, D and E). When using purified, STAR2-pretreated T reg cells to suppress the proliferation of polyclonally activated T con cells, we could not observe differences in the suppressive activity on a per cell basis compared with untreated T reg cells (Fig. 3 F).

The increase in T reg cells observed in our in vitro experiments was furthermore not the result of T reg cell conversion from naive $CD4^+$ cells (Fig. 3 G, left). Indeed, induced T reg (iT reg) cell numbers even decreased significantly in the presence of STAR2 (Fig. 3 G, right).

A human TNFR2-specific STAR2 equivalent expands human T reg cells in vitro

To test for the effects of selective TNFR2 activation on human T reg cells and to prove the potential applicability of our strategy to patients, we isolated $CD4^+$ T cells from PBMCs of healthy donors and treated the cells in vitro with TNC-scTNF(143N/145R), a human TNFR2-specific STAR2 equivalent based on human TNF that has been described elsewhere in detail (Rauert et al., 2010). These experiments revealed a statistically significant expansion of $CD4^+Foxp3^+$ T reg cells in human $CD4^+$ T cell cultures, indicating that TNFR2-mediated T reg cell expansion is not species specific (Fig. 4 A). Furthermore, immunofluorescent staining of large bowel biopsies from allo-HCT patients revealed that the majority of $Foxp3^+$ cells in this GvHD target organ express TNFR2 (Fig. 4 B).

STAR2 expands T reg cells in vivo

To assess the effects of our TNFR2 agonist on mouse T reg cells in vivo, we treated albino B6.Foxp3.Luci.DTR-4 mice, which express firefly luciferase under the control of the Foxp3 promoter, for 2 wk with STAR2 and observed increased T reg cell–derived bioluminescence signals in the whole animal starting 4 d after the initiation of treatment (Fig. 5 A). Ex vivo imaging (Fig. 5 B) and immunofluorescence microscopy (Fig. 5, C and D) proved that there were increased T reg cell numbers in both secondary lymphoid and peripheral organs of STAR2-treated wild-type mice. This included the small bowel, one of the major target organs in GvHD (Welniak et al., 2007; Li and Sykes, 2012). The STAR2-induced increase in T reg cell numbers was not observed in TNFR2-deficient mice (Fig. 5 D). STAR2 treatment significantly increased the

was assessed by flow cytometry. Combined data are from three independent experiments. (D) CD4 T cells were purified from spleens of wild-type, TNF KO, TNFR1 KO, TNFR2 KO, or TNFR1/R2 KO B6 mice, stained with CFSE, and treated with STAR2 for 96 h. CFSE dilution in T reg cells and T con cells was assessed by flow cytometry. Representative data are from three independent experiments. (E) B6.Foxp3.Luci.DTR-4 $CD4^+/CD8^+$ T cells treated with STAR2 for 96 h were analyzed for activation marker expression on $CD4^+Foxp3\text{-}eGFP^-$ T con cells and $CD4^+Foxp3\text{-}eGFP^+$ T reg cells. Representative data are from three independent experiments. (F) B6.Foxp3.Luci.DTR-4 CD4 T cells were treated with STAR2, IL-2, and rapamycin alone or in combination for 96 h and analyzed for CD4 and Foxp3-eGFP expression. Combined data are from four independent experiments. (G) B6.Foxp3.Luci.DTR-4 $CD4^+/CD8^+$ T cells were treated with STAR2 in the presence or absence of IL-2–blocking antibodies (αIL-2) for 96 h and analyzed for CD4 and Foxp3-eGFP expression. Combined data are from seven independent experiments. (B, C, F, and G) Data are mean ± SEM. (H) B6.Foxp3.Luci.DTR-4 or BALB/c $CD4^+/CD8^+$ T cells were treated with STAR2 in the presence or absence of IL-2–blocking antibodies for 96 h and analyzed for proliferation (CellTrace Violet dilution). Representative data are from four independent experiments. (I) Wild-type B6 CD4 T cells were treated with STAR2 and IL-2 alone or in combination for 96 h and analyzed for CD4 and Foxp3 expression and STAT5 phosphorylation. Representative data are from three independent experiments. (J) B6.Foxp3.Luci.DTR-4 or BALB/c $CD4^+/CD8^+$ T cells were treated with STAR2 in the presence or absence of IL-2–blocking antibodies for 96 h and analyzed for activation marker expression on $CD4^+Foxp3\text{-}eGFP^+$ T reg cells. Representative data are from four independent experiments. *, $P \leq 0.05$; **, $P \leq 0.01$, two-tailed unpaired Student's *t* test.

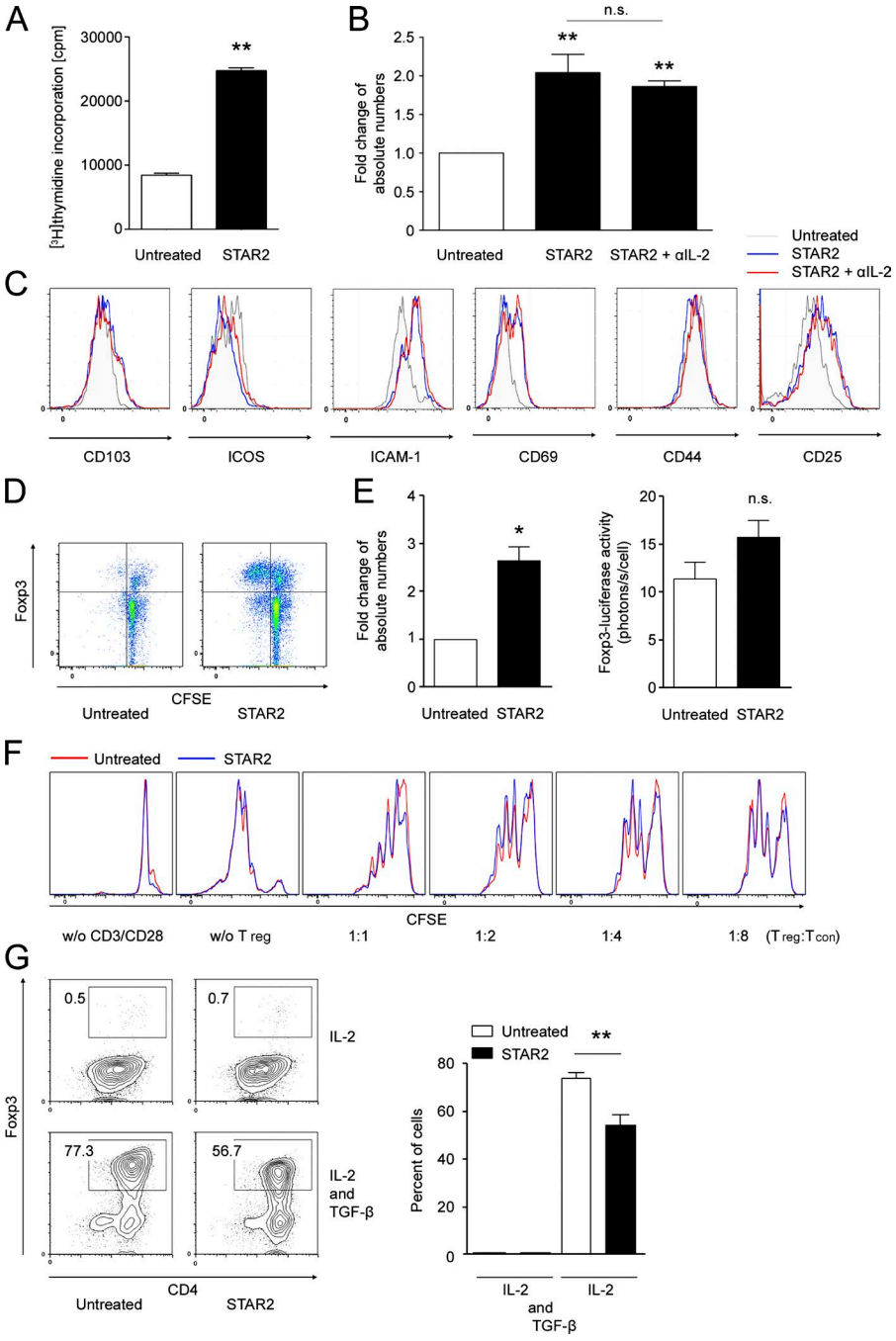

Figure 3. **STAR2 expands purified T reg cells but neither modifies T reg cell suppressive activity on a per cell basis nor induces the conversion of T reg cells from T con cells.** (A) [^{3}H]thymidine incorporation into purified wild-type B6 T reg cells upon STAR2 exposure for 72 h. Data show quadruplicate culture of cells pooled from seven mice. (B) Purified B6.Foxp3.Luci.DTR-4 CD4$^+$CD25$^+$ T reg cells were treated with STAR2 for 96 h and quantified by flow cytometry. Combined data are from three independent experiments. (C) Purified B6.Foxp3.Luci.DTR-4 CD4$^+$CD25$^+$ T reg cells were treated with STAR2 in the presence or absence of IL-2–blocking antibodies (αIL-2) for 96 h and analyzed for the expression of activation markers on CD4$^+$Foxp3-eGFP$^+$ T reg cells. Representative data are from three independent experiments. (D) Wild-type CD4$^+$ T cells were isolated, labeled with CFSE, and either left untreated or treated with 1.67 nM STAR2 for 96 h. Cells were analyzed by flow cytometry for Foxp3 expression and CFSE dilution after gating on CD4$^+$ cells. Representative data are from three independent experiments. (E) B6.Foxp3.Luci.DTR-4 CD4$^+$/CD8$^+$ T cells were treated with 1.67 nM STAR2 for 96 h, and the T reg cell (CD4$^+$Foxp3-eGFP$^+$) numbers in the cultures were assessed by flow cytometry. Foxp3-luciferase expression was analyzed by BLI, and the luciferase activity mirroring the activity of the Foxp3 promoter per cell was determined. Combined data are from eight independent experiments. (F) Wild-type T reg cells were purified, treated overnight with STAR2 or left untreated, and then co-cultured with CD3/CD28-activated, CFSE-labeled T con cells for 72 h to assess the suppressive activity of T reg cells. Representative data are from two independent experiments. (G) CD4$^+$CD25$^-$ T con cells were stimulated with αCD3, αCD28, and IL-2 for 72 h in the presence or absence of TGF-β and STAR2. Combined data are from three or seven independent experiments. (A, B, E, and G) Data are mean ± SEM. *, $P \leq 0.05$; **, $P \leq 0.01$, two-tailed unpaired Student's *t* test. n.s., not significant.

numbers of Ki67$^+$CD4$^+$Foxp3$^+$ cells in the mesenteric lymph nodes, suggesting that it acts by inducing T reg cell proliferation (Fig. 5 E). T reg cells expressed more TNFR2 than conventional CD4$^+$ T cells or CD8$^+$ T cells in the spleen and small intestine, and the expression of TNFR2 increased on T reg cells upon in vivo STAR2 exposure (Fig. 5 F). We also tested the effects of STAR2 on the expression of activation markers on T reg cells and T con cells and found preferential up-regulation of CD103, ICAM-1, and CD44 on splenic T reg cells after in vivo STAR2 treatment. ICOS expression was induced on both T con cells and T reg cells, whereas CD69 expression was not influenced by STAR2 in vivo (Fig. 5 G).

STAR2 does not confer proinflammatory side effects in immunologically naive mice

STAR2 did not activate TNFR1 in vitro (Fig. 1), and it did not pronouncedly influence the proliferation and activation status of T con cells in vitro or in vivo (Figs. 2 and 5). To rule out that our TNFR2 agonist conferred proinflammatory side effects in vivo, we analyzed immunologically naive

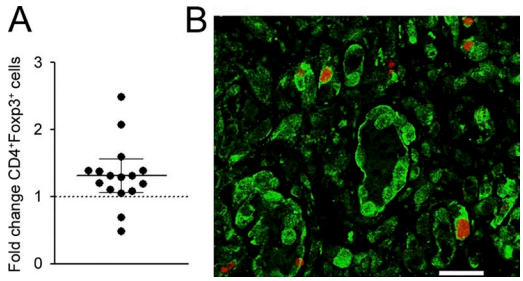

Figure 4. **A human TNFR2-specific STAR2 equivalent expands human T reg cells in vitro.** (A) Human CD4+ T cells were isolated from healthy donor PBMCs and treated with 1.67 nM TNC-scTNF(143N/145R) for 96 h. Combined data are from 16 independent experiments and show mean ± 95% confidence interval. (B) Large bowel biopsies from allo-HCT patients stained for TNFR2 (green) and Foxp3 (red); representative image from five patients. Bar, 25 µm.

mice treated with STAR2. The treatment showed no effect on other lymphocyte subsets besides T reg cells, whereas it changed the composition of the myeloid compartment in the spleen and lungs (Fig. 6 A). Importantly, STAR2 application over the course of 2 wk had no effect on body weight (bw; Fig. 6 B), and it did not affect serum (Fig. 6 C) or tissue levels (Fig. 6 D) of IL-6, IL-10, MCP-1, IFN-γ, TNF, and IL-12.

STAR2 pretreatment protects allo-HCT–recipient mice from acute GvHD

Next, we tested whether prophylactic TNFR2 activation–mediated expansion of T reg cells in allo-HCT recipients protects them from acute GvHD. T reg cells have been reported to be highly radiation resistant compared with other immune cells (Anderson et al., 2004; Komatsu and Hori, 2007), and radiation-resistant T reg cells have been reported to control chronic GvHD in mice (Komatsu and Hori, 2007). Approximately half of the initial T reg cell numbers in lethally irradiated albino B6.Foxp3.Luci.DTR-4 mice rescued with wild-type bone marrow persisted 3 wk after transplantation based on bioluminescence imaging (BLI) of luciferase-expressing host T reg cells (Fig. 7, A and B) and flow cytometry (Fig. 7 C), demonstrating radiation resistance of these cells in our model, too.

STAR2 pretreatment significantly prolonged the survival of fully MHC-mismatched allo-HCT recipients (FVB[H-2^q]→C57BL/6[H-2^b]; Fig. 7 D), increasing the median survival from 16 d to >40 d compared with untreated recipients. Prolonged survival was associated with reduced weight loss (Fig. 7 E) and lower clinical scores (Fig. 7 F). However, when host T reg cells were eliminated from albino B6.Foxp3.Luci.DTR-4 mice by diphtheria toxin (DTx) treatment before transplantation (Fig. 7, D–F) or when recipient mice were deficient for TNFR2 (Fig. 7, G–I), the protective effect of STAR2 was completely abrogated. In a second MHC-mismatched allo-HCT model (C57BL/6[H-2^b]→BALB/c[H-2^d]), STAR2-pretreated mice also lived significantly longer than control mice (Fig. 7 J), with a median survival of 21 versus 10 d. They lost less weight after allo-HCT (Fig. 7 K) and had lower clinical scores (Fig. 7 L).

STAR2 protects from GvHD by reducing early alloreactive donor T cell expansion and tissue destruction without modulating myeloid-derived suppressor cells (MDSCs)

BALB/c allo-HCT–recipient mice were transplanted with C57BL/6 wild-type bone marrow and luciferase-expressing T cells. In vivo and ex vivo BLI revealed significantly reduced early donor T cell proliferation and diminished target organ infiltration in STAR2-pretreated mice compared with untreated controls (Fig. 8, A and B). Reduced target tissue infiltration by donor T cells was confirmed by immunofluorescence microscopy (Fig. 8 C) and flow cytometry (Fig. 8 D). STAR2-pretreated mice exhibited less tissue damage and accordingly also lower pathology scores, especially so in the small bowel (Fig. 8 E). These results are in agreement with several studies in which donor T reg cells protected against GvHD in mouse models by suppressing early donor effector T cell proliferation and migration (Hoffmann et al., 2002; Nguyen et al., 2007).

STAR2 pretreatment did not alter the myeloid compartment in either lymphatic or GvHD target organs 6 d after transplantation (Fig. 8 F) and did not modify the suppressive capacity of MDSCs in the spleen or the small bowel (Fig. 8 G).

STAR2 pretreatment does not interfere with GvL activity of transplanted T cells

Next, we tested whether the antitumoral activity of transplanted T cells against co-transplanted, luciferase-expressing A20 (Edinger et al., 2003) or preexisting IM380 (Chopra et al., 2013b) B cell lymphomas was maintained in TNFR2-primed recipients, despite the reduced capacity of donor T cells to induce lethal GvHD. When mice were transplanted with bone marrow only, both lymphoma types grew progressively until the mice succumbed to the malignancies (Fig. 9, A, B, E, and F). When untreated or STAR2-pretreated mice were co-transplanted with allogeneic T cells, tumors were efficiently eradicated in both groups. STAR2-pretreated mice were furthermore protected from lethal acute GvHD (median survival: A20, 38.5 vs. 14.5 d [Fig. 9 B]; IM380, 26 vs. 18 d [Fig. 9 F]). This protection translated to significantly reduced weight loss and lower clinical scores (Fig. 9, C, D, G, and H). Our findings correspond to other studies showing the elimination of A20 and BCL-1 tumor cells after co-transplantation of GvHD-inhibiting amounts of donor T reg cells (Edinger et al., 2003; Nguyen et al., 2007).

STAR2 does not interfere with the immunological clearance of pathogens after transplantation

Expansion of T reg cells for GvHD prophylaxis may raise the concern that the immune control of opportunistic infections (Marr et al., 2002; Hebart and Einsele, 2004) in immunocompromised HCT recipients during immune re-

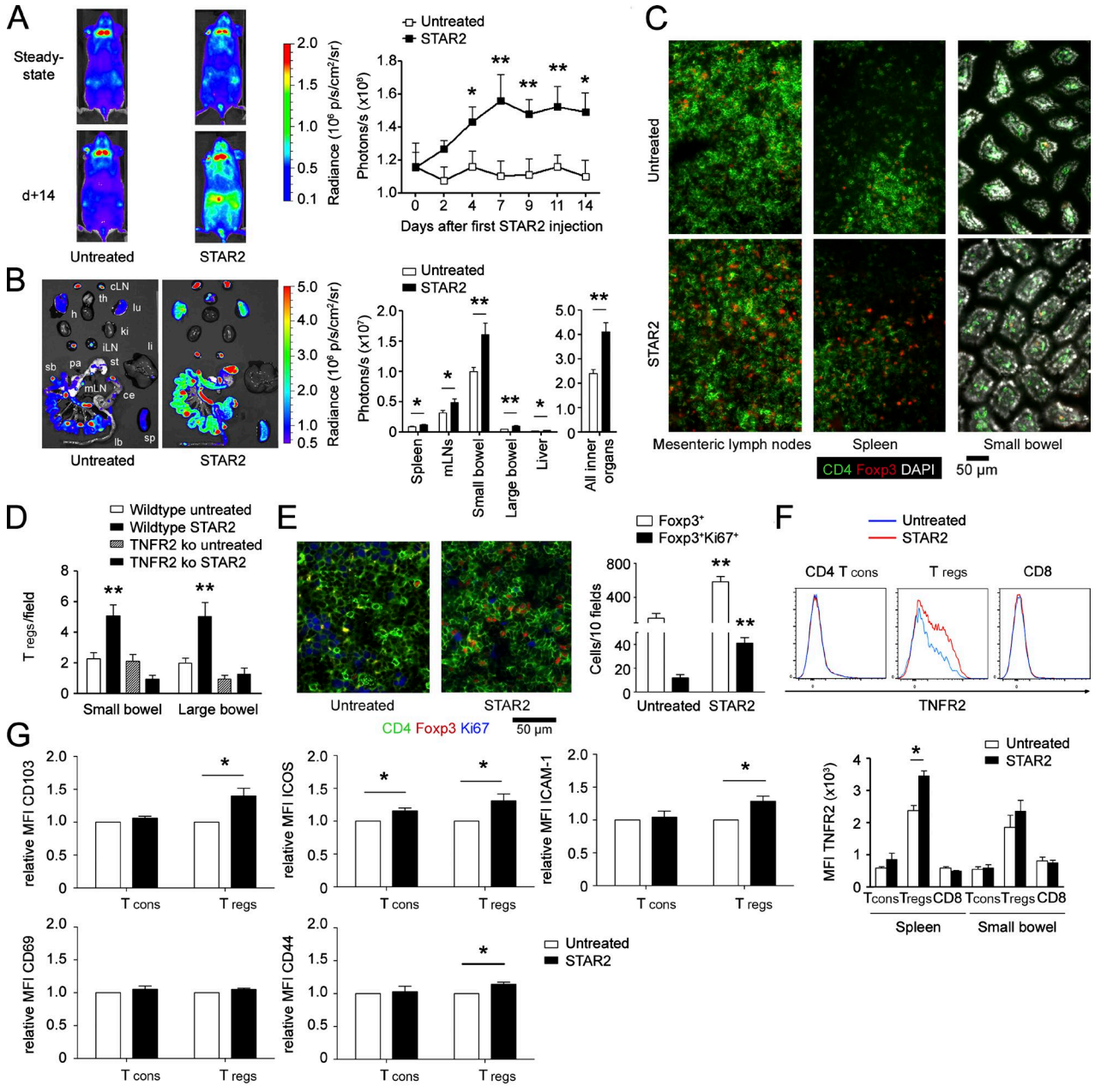

Figure 5. **STAR2 expands T reg cells in vivo.** (A) Albino B6.Foxp3.Luci.DTR-4 mice were treated with 75 µg (416 pM) STAR2 in PBS i.p. on days 0, 2, 4, 7, 9, and 11. T reg cell numbers were evaluated in vivo using Foxp3-driven luciferase activity. Representative images are from 11 untreated and 9 STAR2-treated mice. (B) Ex vivo imaging of internal organs: cervical lymph nodes (cLN), thymus (th), heart (h), lungs (lu), kidneys (ki), inguinal lymph nodes (iLN), liver (li), stomach (st), pancreas (pa), small bowel (sb), mesenteric lymph nodes (mLN), cecum (ce), large bowel (lb), and spleen (sp). Combined data are from 11 untreated and 9 STAR2-treated mice from two independent experiments. (C) Representative microphotographs for $CD4^+Foxp3^+$ cells in small bowel, spleen, and mesenteric lymph nodes of five untreated and three STAR-treated wild-type mice. (D) T reg cells were counted among small and large bowels of untreated ($n = 5$) and STAR2-treated ($n = 3$) wild-type mice and untreated ($n = 4$) and STAR2-treated ($n = 3$) TNFR2 KO mice. Combined data are from two independent experiments. (E) Representative microphotographs and quantification of $CD4^+Foxp3^+Ki67^+$ cells in mesenteric lymph nodes of untreated ($n = 5$) and STAR2-treated ($n = 3$) wild-type mice. Combined data are from two independent experiments. (F) TNFR2 expression on $CD4^+$ T con cells, T reg cells, and $CD8^+$ T cells in the spleen (top and bottom) and the small bowel (bottom only). Representative flow cytometry plots and combined data are from two independent experiments with eight untreated and seven STAR2-treated mice. (G) B6 wild-type mice were treated with STAR2 i.p. for 2 wk, and the expression of activation-associated surface proteins was assessed by flow cytometry on $CD4^+Foxp3^+$ T reg cells and $CD4^+Foxp3^+$ T con cells. Combined data are from two independent experiments with seven untreated and six STAR2-treated mice. (A, B, and D–G) Data are mean ± SEM. MFI, mean fluorescence intensity. *, $P \leq 0.05$; **, $P \leq 0.01$, two-tailed unpaired Student's *t* test.

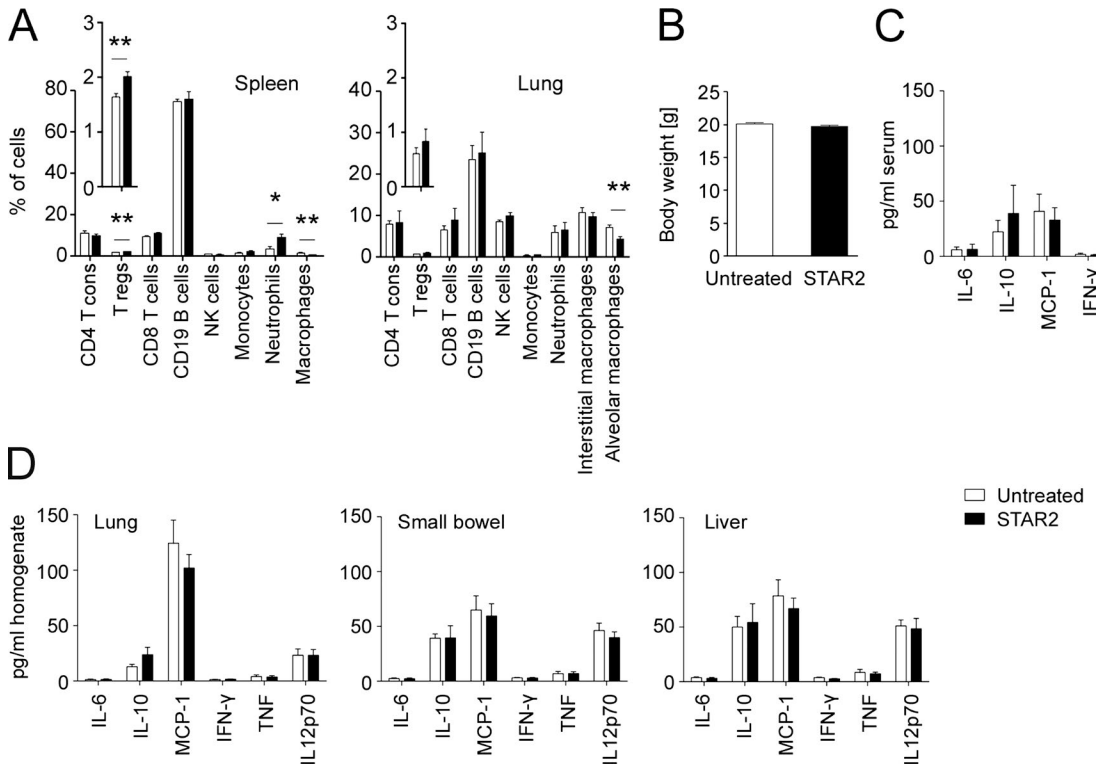

Figure 6. **STAR2 does not confer proinflammatory side effects in immunologically naive mice.** (A) B6 wild-type mice were treated with STAR2 i.p. for 2 wk, and the immune cell composition of the spleen and the lungs was assessed by flow cytometry. Monocytes were identified as $CD11b^{+}Ly6C^{+}Ly6G^{-}$, neutrophils as $CD11b^{+}Ly6C^{+}Ly6G^{+}$, splenic macrophages as $CD11b^{dim}CD11c^{-}CD14^{+}F4/80^{hi}$, interstitial macrophages as $CD11b^{+}CD11c^{-}CD14^{dim}F4/80^{+}$, and alveolar macrophages as $CD11b^{-}CD11c^{hi}CD14^{+}F4/80^{+}$. Combined data are from two independent experiments with five untreated and three STAR2-treated mice *, $P \leq 0.05$; **, $P \leq 0.01$, two-tailed unpaired Student's *t* test. (B) bw's of untreated ($n = 30$) and STAR2-treated ($n = 30$) mice. Combined data are from six independent experiments. (C) Serum samples were collected from STAR2-treated mice and analyzed by cytometric bead array for cytokine levels (untreated, $n = 9$; and STAR2, $n = 9$). Combined data are from three independent experiments. (D) Lung, small bowel, and liver samples were collected from STAR2-treated mice, homogenized, and analyzed by cytometric bead array for cytokine levels (untreated, $n = 6$; and STAR2, $n = 6$). Combined data are from two independent experiments. Data are mean ± SEM.

constitution could be suppressed. We therefore tested the impact of STAR2 pretreatment in mouse models of mouse CMV (mCMV; Podlech et al., 2000, 2002) after experimental HCT. STAR2 pretreatment of HCT recipients did not enhance mCMV infection after syngeneic (Fig. 10, A and B) or after allogeneic HCT (Fig. 10, D and E) and also had no effect on the numbers and the activation status of lung-infiltrating total and mCMV-specific $CD8^{+}$ T cells (Fig. 10 C).

DISCUSSION

Exogenous activation of TNFR2 with the novel mouse TNFR2 agonist STAR2 allows the expansion of T reg cells in vivo and protects allo-HCT recipients from acute GvHD, also sparing antilymphoma and antiinfectious properties of transplanted donor T con cells.

T reg cells prevent excessive alloreactive T cell proliferation in the lymphohematopoietic system. This observation is critical for the mechanistic understanding of how T reg cells can prevent GvHD but still allow functional immune responses against leukemias, lymphomas, and infections (Edinger et al., 2003; Jones et al., 2003; Trenado et al., 2003; Schneidawind et al., 2013, 2014). Of note, leukemias and lymphomas also primarily manifest in the lymphohematopoietic system, and consequently, if T reg cells limit the number of alloreactive effector T cells, the alloimmune response can be predominantly contained to this site (Kim et al., 2003; Beilhack et al., 2005, 2008; Coghill et al., 2010), and the GvL response can be preserved. In settings where there is a relatively high T cell precursor frequency for major and minor alloantigens, expansion of cytotoxic T cells is less important for the exertion of GvL responses. However, in the opposite scenario (e.g., after vaccination to a rare tumor antigen where the T cell precursor frequency is low and T cell expansion is required for a biological effect), T reg cells appear to suppress these immune-mediated antitumor effects (Casares et al., 2010; Klages et al., 2010). Therefore, in the typical allo-HCT setting, which comprises immune activation, e.g., because of host conditioning, often relatively high T cell precursor frequencies for major and minor alloantigens and low tumor burden (minimal residual disease) appear to be an ideal setting to foster T reg cell function for therapeutic benefits.

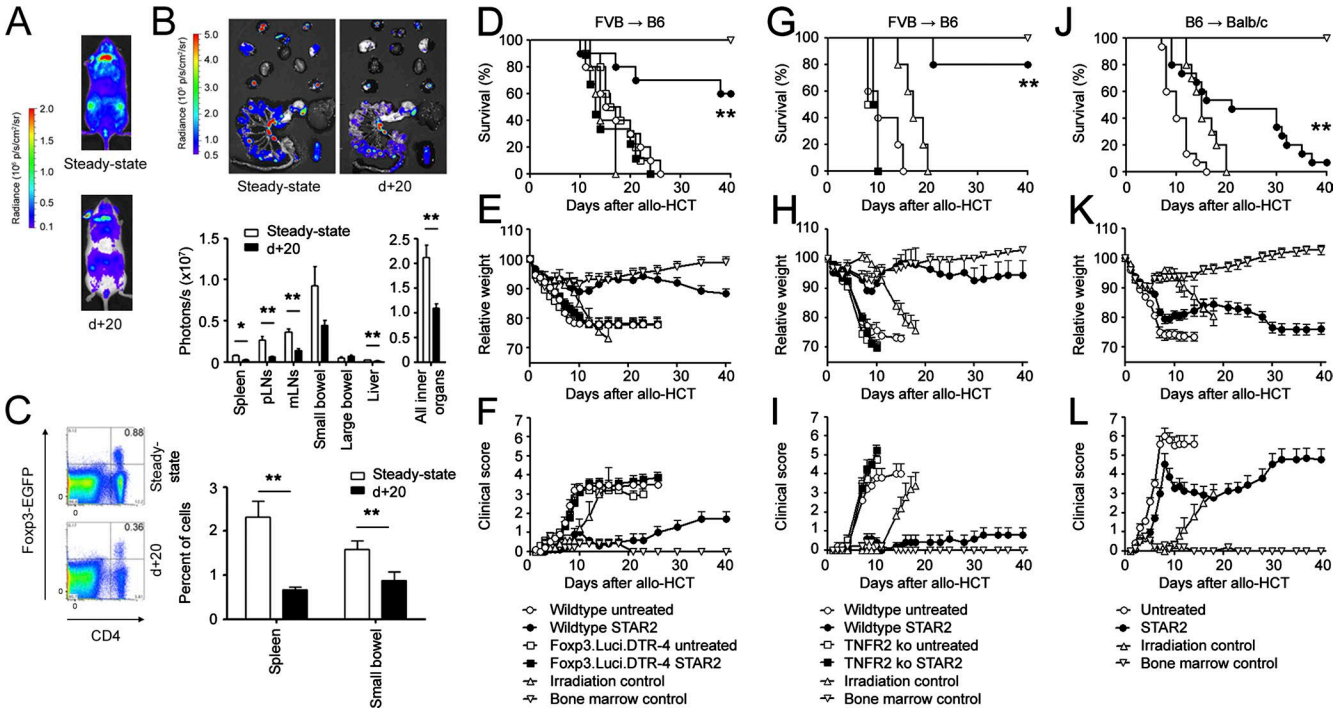

Figure 7. **STAR2 pretreatment protects allo-HCT recipient mice from acute GvHD.** (A–C) Albino B6.Foxp3.Luci.DTR-4 mice were lethally irradiated with 9 Gy and transplanted with 5×10^6 B6 wild-type bone marrow cells. *, $P \leq 0.05$; **, $P \leq 0.01$, two-tailed unpaired Student's *t* test. (A) Representative in vivo BLI images of Foxp3-driven luciferase activity before and 20 d after syngenic bone marrow transfer from five mice per group are shown. (B, top) Representative ex vivo BLI images of Foxp3-driven luciferase activity of internal organs before and 20 d after syngenic bone marrow transfer from five mice per group. (Bottom) Quantification of ex vivo BLI data. Combined data are from two independent experiments with five mice per group and show mean ± SEM. mLN, mesenteric LN; pLN, peripheral LN. (C, left) Representative flow cytometry plots of $CD4^+Foxp3\text{-}eGFP^+$ cells among live $CD45.2^+$ immune cells in the spleen before and 20 d after bone marrow transfer from five mice per group. (Right) Quantification of $CD4^+Foxp3\text{-}eGFP^+$ cells among live $CD45.2^+$ immune cells in the spleen and small bowel. Combined data are from two independent experiments with five mice per group and show mean ± SEM. (D–F) Albino B6.Foxp3.Luci.DTR-4 mice and their wild-type littermates ($H\text{-}2^b$) were treated with STAR2 i.p. for 2 wk and injected with 15 ng DTx/g bw on days 2 and 1 before allo-HCT with 5×10^6 FVB/N ($H\text{-}2^q$) bone marrow cells and 10^6 FVB/N ($H\text{-}2^q$)-enriched T cells (wild type untreated, $n = 10$; wild type STAR2, $n = 10$; Foxp3.Luci.DTR-4 untreated, $n = 10$; Foxp3.Luci.DTR-4 STAR2, $n = 9$; irradiation control, $n = 5$; and bone marrow control, $n = 5$). Combined data are from two independent experiments. (D) Survival. (E) Relative weight change. (F) Clinical scoring. (G–I) B6 wild-type and TNFR2 KO mice ($H\text{-}2^b$) were treated with STAR2 i.p. for 2 wk before allo-HCT with 5×10^6 FVB/N ($H\text{-}2^q$) bone marrow cells and 10^6 FVB/N ($H\text{-}2^q$)-enriched T cells (wild type untreated, $n = 5$; wild type STAR2, $n = 5$; TNFR2 KO untreated, $n = 4$; TNFR2 KO STAR2, $n = 4$; irradiation control, $n = 5$; and bone marrow control, $n = 5$). Combined data are from two independent experiments. (G) Survival. (H) Relative weight change. (I) Clinical scoring. (J–L) BALB/c mice ($H\text{-}2^d$) were treated with STAR2 i.p. for 2 wk before allo-HCT with 5×10^6 B6 ($H\text{-}2^b$) bone marrow cells and 10^6 luc^+ B6.L2G85.CD90.1 ($H\text{-}2^b$)-enriched T cells (untreated, $n = 15$; STAR2, $n = 15$; irradiation control, $n = 10$; and bone marrow control, $n = 10$). Combined data are from three independent experiments. (J) Survival. (D, G, and J) **, $P \leq 0.01$, log-rank test. (K) Relative weight change. (L) Clinical scoring. Data are mean ± SEM.

The positive effects of TNFR2 activation on mouse T reg cells are convincing throughout the literature (Chen et al., 2007, 2008, 2013; Grinberg-Bleyer et al., 2010; Housley et al., 2011; Chopra et al., 2013a), whereas the effects of TNF on human T reg cells are less clear. In our present study, we show that a human TNFR2 agonist expands human T reg cells in vitro. Chen et al. (2010a) reported earlier that TNFR2 is a marker associated with increased suppression by human peripheral blood T reg cells, and recently, it was demonstrated that both an agonistic antibody for TNFR2 and a cross-linked TNF multimer, which would also activate TNFR1, efficiently expanded T reg cells from healthy donors in vitro (Okubo et al., 2013; Ban et al., 2015).

Other studies have demonstrated that activation of TNFR2 on human T reg cells inhibits their suppressive functions. Nagar et al. (2010) and Valencia et al. (2006) demonstrated the activation of TNFR2 signaling in human T reg cells to inhibit the suppression of T con cell proliferation by these cells. Of note, in both studies, the authors used polyclonal stimulation (anti-CD3) to activate the T con cells in culture. Valenica et al. (2006) furthermore characterized T reg cells from patients with rheumatoid arthritis and found decreased suppression by these cells, whereas they observed an increase in the suppressive activity of T reg cells isolated after TNF blocking therapy. Similar results were obtained from a different group (Ehrenstein et al., 2004) showing that TNF blockade in rheumatoid

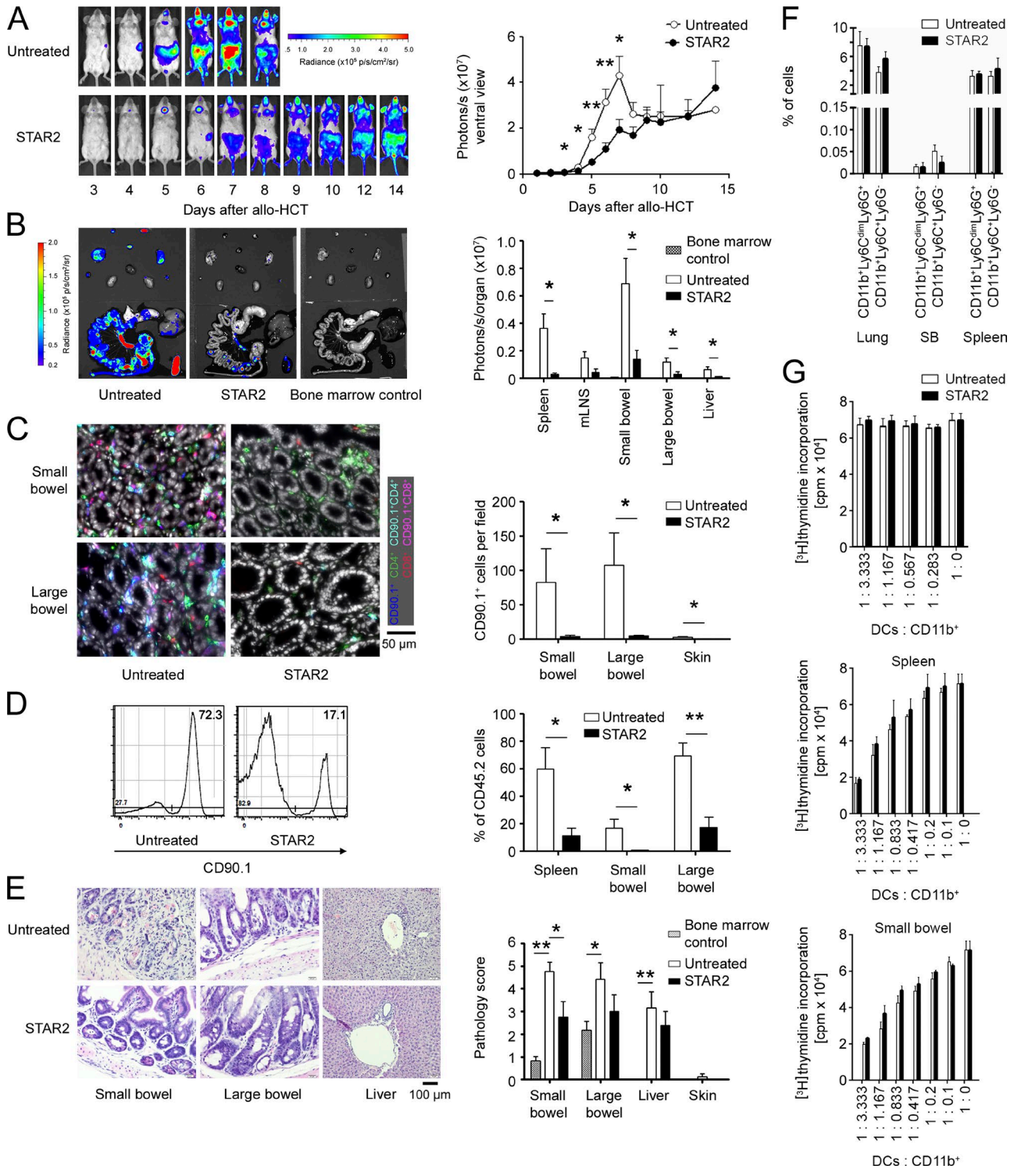

Figure 8. **STAR2 protects from GvHD by reducing early alloreactive donor T cell expansion and tissue destruction without modulating MDSCs.** (A–E) BALB/c mice (H-2^d) were treated with STAR2 i.p. for 2 wk before allo-HCT with 5 × 10^6 B6 (H-2^b) bone marrow cells and 10^6 B6.L2G85.CD90.1 (H-2^b)-enriched T cells. (A) Representative in vivo BLI images and quantification of luc$^+$ donor T cell expansion and migration in transplanted mice (untreated, n = 15; and STAR2, n = 15). Combined data are from three independent experiments and show mean ± SEM. (B–E) On day 6 after allo-HCT, recipient mice were dissected. (B) Internal organs were imaged ex vivo for donor T cell–derived bioluminescence (untreated, n = 5; STAR2, n = 5; and bone marrow control, n = 5). Combined data are from two independent experiments. mLN, mesenteric LN. (C) Internal organs were prepared for immunofluorescence microscopy for the expression of CD90.1, CD4, and CD8 (untreated, n = 5; and STAR2, n = 5). Combined data are from two independent experiments.

arthritis patients reverses the observed suppression defect of isolated T reg cells. In a follow-up study, it was demonstrated that newly occurring T reg cells after TNF blocking therapy are actually iT reg cells and not nT reg cells (Nadkarni et al., 2007). These results are in line with our own results, i.e., that TNFR2 activation induces mouse nT reg cells but inhibits the induction of iT reg cells from T con cells. Other investigators also demonstrated that TNF blocks iT reg cell conversion in mice (Housley et al., 2011; Zhang et al., 2013).

We propose that STAR2 likely affects T reg cells in several distinct ways. Some of the effects possibly involve or at least require the presence of IL-2 and the help of T con cells, whereas other effects appear to be solely T reg cell intrinsic and do not require IL-2. STAR2 expands T reg cells both in mixed T cell and purified T reg cell cultures, calling for this to be a T reg cell–intrinsic effect. We found the induction of activation markers on T reg cells to be independent of the presence of IL-2, whereas it is vital for the expansion and proliferation of these cells in mixed cultures. The observation that STAR2 induces several markers on T reg cells both in the presence and absence of T con cells, whereas it only up-regulates other markers in the presence of T con cells, speaks for T con cell support to be involved in this effect. Another reason could as well be that the cell density of in vitro cultures plays a role in our observed discrepancies between mixed T cell cultures and purified T reg cell cultures (Römer et al., 2011). The failure of in vitro STAR2-treated T reg cells to be more suppressive than untreated T reg cells may be the result of the experimental conditions, i.e., that the absence of T con cells prevents the T reg cells from becoming fully activated by STAR2. However, it might be that despite up-regulating activation markers, the STAR2-treated T reg cells are not more functional than untreated cells but that their immunosuppressive effects in our in vivo model are the result of increased numbers rather than increased function on a per cell basis.

It is worth noting that TNF blockade is associated with the exacerbation of various other autoimmune diseases in human patients (Robinson et al., 2001; Ramos-Casals et al., 2008; Ko et al., 2009), stressing the fact that TNF indeed has the potential to act as an immunosuppressive factor, possibly depending on the underlying disease and whether nT reg cells or iT reg cells are the main immunosuppressive T cells in the respective disease setting.

We and others have demonstrated that TNFR2 functions as a co-stimulatory molecule for T reg cells. Chen et al. (2010b) have additionally shown that TNFR2 is also expressed on a subset of T con cells and that these cells respond to TNF. TCR engagement of T con cells induces TNFR2 expression, indicating that activated T con cells respond more to TNF than naive T cells (Chen et al., 2010b). We only detected very weak expression of TNFR2 on a subset of CD4 T con cells, and TNFR2 activation by STAR2 conferred very minor effects to T con cells in terms of activation marker expression and proliferation. Exogenous treatment of healthy mice with STAR2 did not cause adverse effects, indicating that TNFR2 activation in our model does not activate proinflammatory signaling in conventional T cells. There could be several reasons for this: (a) the low expression of TNFR2 on these cells is not sufficient to switch on downstream signaling, (b) T reg cells outcompete T con cells for STAR2 in vivo because of their much higher TNFR2 expression, or (c) STAR2-expanded and -activated T reg cells actively suppress activated T con cells in our model. Indeed, the fact that TCR-activated T con cells may robustly respond to TNFR2 co-stimulation was the reason why we chose to treat allo-HCT recipient mice with STAR2 for 2 wk before the actual transplantation to minimize potential effects of TNFR2 engagement of allogenically activated T con cells.

Our therapeutic approach using donor T reg cells for the preventive treatment of GvHD has further advantages over current clinical protocols, as it demands neither Good Manufacturing Practice–compliant production nor ex vivo expansion of donor cells with the potential risk of functional loss. Furthermore, T reg cells are expanded in vivo within GvHD target tissues, as opposed to transplanted T reg cells that would first need to home to these sites. Human mucosal T reg cells that homed to the intestinal tract of patients after allo-HCT expressed TNFR2 and TNC-scTNF(143N/145R), a human TNF-based STAR2 variant specific for human TNFR2-expanded T reg cells in vitro. These observations indicate the potential of our strategy to protect allo-HCT patients from acute GvHD by expanding TNFR2-positive T reg cells via selective TNFR2 activation in vivo. Furthermore, this strategy appears to be beneficial for other pathological settings in which elevated numbers of T reg cells are desirable, such as autoimmune diseases and solid organ transplantation.

(D) Internal organs were prepared for flow cytometry (cells were gated on live CD45.2$^+$ immune cells and analyzed for CD90.1 expression–representing donor T cells; untreated, $n = 5$; and STAR2, $n = 5$). Combined data are from two independent experiments. (E) Internal organs were assessed for tissue damage after hematoxylin/eosin staining (untreated, $n = 8$; STAR2, $n = 8$; and bone marrow control, $n = 6$). Combined data are from three independent experiments. (F) B6 wild-type mice (H-2^b) were treated with STAR2 i.p. for 2 wk, and MDSCs in the lungs, the small bowel (SB), and spleen were assessed by flow cytometry 6 d after allo-HCT with 5×10^6 FVB (H-2^q) BM cells and 10^6 FVB (H-2^q) T cells (untreated, $n = 3$; and STAR2, $n = 3$). Representative data are from two independent experiments. (G) CD11b$^+$ cells were isolated from either the spleen or the small bowel of STAR2-treated B6 mice before (top) or after (middle and bottom) allogeneic transplantation. Cells of three animals were pooled for analysis. Triplicates of 3×10^5 lymph node cells from BALB/c mice as a source of responder T cells were cultured together with 3×10^4 LPS-matured allogeneic DCs from B6 mice and different numbers of sorted B6 MDSCs. After 3 d, cells were pulsed with [^{3}H]thymidine overnight to measure cell proliferation. Representative data are from two independent experiments. Data are mean ± SEM. *, $P \leq 0.05$; **, $P \leq 0.01$, two-tailed unpaired Student's *t* test.

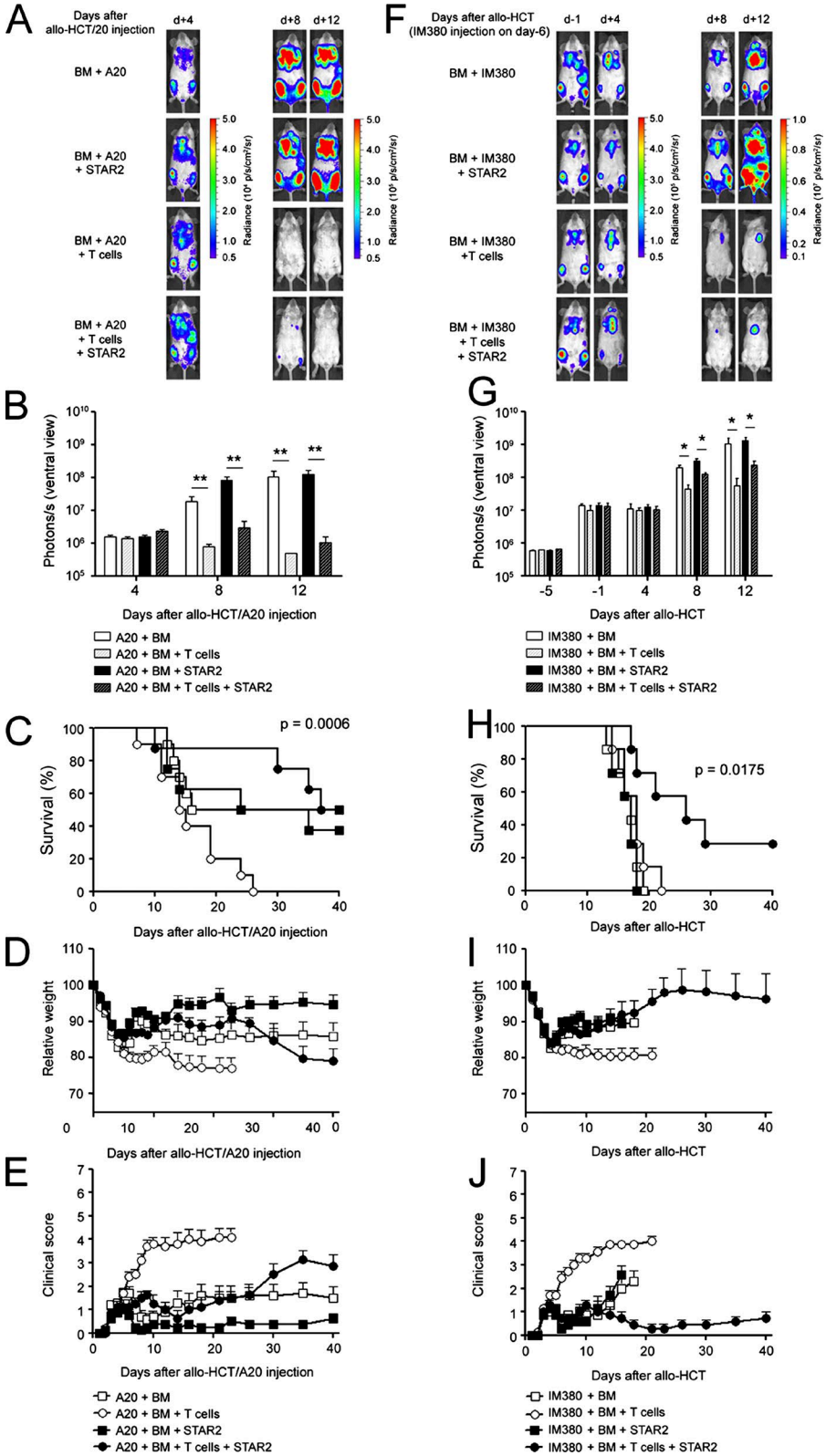

Figure 9. **STAR2 pretreatment does not interfere with GvL properties of transplanted T cells.** (A–E) BALB/c (H-2^d) mice were treated with STAR2 i.p. for 2 wk before allo-HCT. Lethally irradiated mice were injected i.v. with 10^5 luciferase-expressing A20 B cell lymphoma cells (H-2^d) and transplanted with 5×10^6 B6 (H-2^b) bone marrow cells. To induce GvHD, 10^6 B6 (H-2^b)-enriched T cells were injected i.v. (A20 + BM, $n = 10$; A20 + BM + T cells, $n = 10$; A20 + BM + STAR2, $n = 8$; and A20 + BM + T cells + STAR2, $n = 8$). Combined data are from two independent experiments. (A) Representative in vivo BLI images. (B) Graphic evaluation of BLI images taken from a ventral view. **, $P \leq 0.01$, two-tailed unpaired Student's t test. (C) Survival using log-rank test. (D) Relative weight change. (E) Clinical scoring. (F–J) BALB/c (H-2^d) mice were treated with STAR2 i.p. for 2 wk before allo-HCT. Mice were injected i.v. with 10^5 luciferase-expressing IM380 B cell lymphoma cells (H-2^d) 6 d before allo-HCT. Lethally irradiated mice were transplanted with 5×10^6 B6 (H-2^b) bone marrow cells. To induce GvHD, 10^6 B6 (H-2^b)-enriched T cells were injected i.v. (IM380 + BM, $n = 7$; IM380 + BM + T cells, $n = 7$; IM380 + BM + STAR2, $n = 7$; and IM380 + BM + T cells + STAR2, $n = 7$). Combined data are from two independent experiments. (F) Representative in vivo BLI images. (G) Graphic evaluation of BLI images taken from a ventral view. *, $P \leq 0.05$, two-tailed unpaired Student's t test. (H) Survival using log-rank test. (I) Relative weight change. (J) Clinical scoring. Data are mean ± SEM.

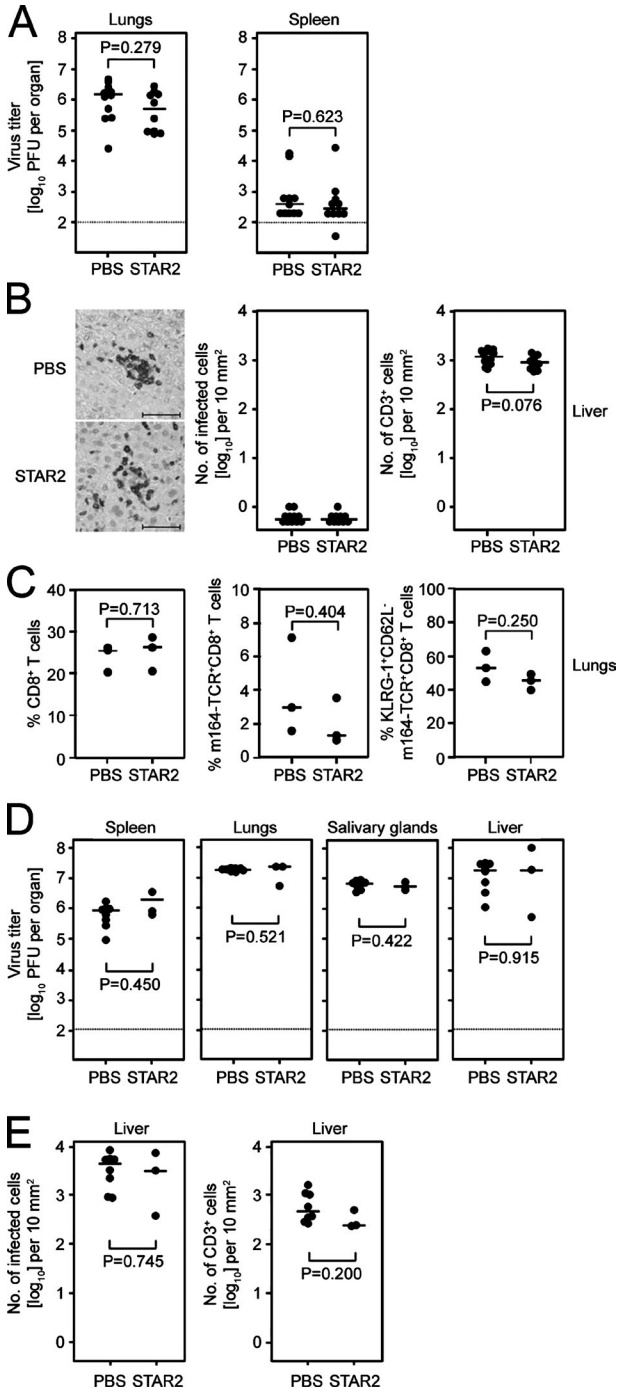

Figure 10. **STAR2 does not interfere with the immunological clearance of mCMV infection after transplantation.** (A–C) BALB/c (H-2^d) recipients of syngenic HCT were pretreated with STAR2 for 2 wk and analyzed 4 wk after HCT and infection. (A) Infectious virus (expressed as PFU) in lungs and spleen. (B) Immunohistochemical detection of infected cells (red stain) and CD3ε^+ infiltrate lymphocytes (black stain) in liver tissue sections. Please note that there are no infected red cells visible because the infection is controlled in both groups at this point. (Left) Representative images. Bars, 50 µm. (Middle and right) Quantification of infected cells (middle) and of infiltrating CD3ε^+ lymphocytes (right). (A and B) Symbols represent individual mice. Median values are marked (PBS, $n = 11$; and STAR2, $n = 10$). Combined data are from two independent experiments. The dotted line shows the detection limit. (C) Cytofluorometric quantitation and characterization of pulmonary CD8 T cells. (Left) Percentage of CD8 T cells in the lymphocyte gate. (Middle) Percentage of viral m164 epitope–specific cells among the CD8 T cells. (Right) Percentage of short-lived effector cells among the m164 epitope–specific CD8 T cells. Symbols represent three independent pools, each composed of cells from three to four mice representing their experimental mean. (D and E) BALB/c (H-2^d) recipients of allo-HCT (with BALB/c-H-2^{dm2} mice as donors) were pretreated with STAR2 for 2 wk and analyzed 18 d after HCT (PBS, $n = 8$; and STAR2, $n = 3$). Combined data are from two independent experiments. (D) Infectious virus (expressed as PFU) in spleen, lungs, salivary glands, and liver. (E) Immunohistochemical detection and quantification of infected cells (left) and of infiltrating CD3ε^+ lymphocytes (right). (A–E) Two-tailed unpaired Student's *t* test was used. All p-values were calculated with Welch's correction to account for unequal variance. Data from exponential growth curves (virus titers and numbers of infected cells) were log-transformed for the Student's *t* test.

MATERIALS AND METHODS

In silico modeling of TNF–TNFR interactions

The ligand–receptor complexes of mouse TNF bound to the extracellular domains of mouse TNFR1 and mouse TNFR2 were modeled using the structures of human lymphotoxin-α bound to TNFR1 and human TNF bound to TNFR2 as templates. In brief, the amino acid sequences of the human and mouse TNFR1 ectodomains were aligned using CLU STALW software and the structure of human TNFR1 (PDB accession no. 1TNR, chain R). Different amino acids in the template were replaced with those of mouse TNFR1 using the tool ProteinDesign in the software package Quanta2008 (MSI Accelrys). Insertions and deletions were modeled manually using main chain torsion angles within the allowed areas of the Ramachandran plot. Rotamer searches for the side chain torsion angles were performed to minimize clashes between side chains of introduced amino acid residues. The model structure was refined by energy minimization (500 steps per minimization run) using the CHARMM27 all-hydrogen force field using only geometric energy terms and the conjugate gradient algorithm. First, only hydrogen atoms were allowed to move, and then side chain atoms were released, but the atom movements were restricted by applying a harmonic potential of 25 kcal mol^{-1} Å^{-2}, which was gradually lowered (5 kcal mol^{-1} Å^{-2} and 0 kcal mol^{-1} Å^{-2}). Finally, the structure was refined by performing a final energy minimization with only the main chain atoms being restrained by a weak harmonic potential (2 kcal mol^{-1} Å^{-2}). The structures of the mouse TNF (PDB accession no. 3ALQ, chain A) and mouse TNFR2 (PDB accession no. 3ALQ, chain R) ectodomains were obtained accordingly. The binary ligand–receptor complexes were formed by docking the structure models onto the structure of the TNF–TNFR complexes of LTα–TNFR1 and TNF–TNFR2 (PDB accession nos. 1TNR and 3ALQ, respectively). All models displayed good backbone and side chain geometries without bad van der Waals contacts.

TNFR2-specific variants of mouse TNF were designed using information previously published (Loetscher et al., 1993) on TNFR2-specific mutants of human TNF and modeling these amino acid exchanges in the models described in the previous paragraph.

Cloning and production of recombinant proteins

Expression constructs encoding secretable Flag-tagged *Gaussia princeps* luciferase (GpL)–TNC–mouse TNF and Flag-tagged TNC–sc–mouse TNF were generated by in-frame insertion of amplicons encoding mouse TNF (aa 91–235) or single-chain mouse TNF (aa 91–235) to the 3′ ends of GpL-Flag-TNC and Ig-leader Flag-TNC expression cassettes previously cloned into the pCR3 vector. An expression plasmid containing a single-chain mouse TNF (aa 91–235) DNA cassette in which three mouse TNF (aa 91–235)–encoding domains were linked by $(GGGS)_4$ peptide linker–encoding sequences served as a template for generating the amplicons (provided by P. Scheurich and K. Pfizenmaier, Institute of Immunology and Cell Biology, University of Stuttgart, Stuttgart, Germany). To obtain the mouse TNFR2–specific variants GpL-STAR2 and Flag-tagged STAR2, synthetic genes encoding conventional mutant mouse TNF(D221N-A223R) or single-chain mutant mouse TNF(D221N-A223R) were obtained from a commercial supplier (Geneart) and inserted into the pCR3-based GpL-Flag-TNC and Ig-leader Flag-TNC expression vectors. The combined use of the trimerization domain of chicken TNC and three peptide linker–connected TNF protomers results in the formation of a molecule with three covalently linked TNF trimers that, in contrast to conventional trimeric TNF molecules, both binds TNFR2 and triggers robust receptor activation.

To produce the TNF variants, HEK293 cells were transiently transfected with the corresponding expression plasmids via electroporation with an electroporator (Easyject Plus; PeqLab) and cultivated for 5–7 d, supernatants were purified using anti-Flag affinity chromatography, and the concentrations of the recombinant proteins were determined by anti-Flag Western blotting and comparison with a Flag-tagged standard protein.

Binding studies

To analyze the binding of wild-type mouse TNF and mouse STAR2 to mouse TNFR2, HEK293 cells were electroporated with an empty vector or a mouse TNFR2 expression plasmid. The next day, transfected cells were seeded into 24-well plates. After an additional day, the cells were incubated pairwise at 37°C for 2 h with increasing concentrations of GpL-TNC–mouse TNF and GpL-STAR2, and cell-bound luciferase activity was assayed using the *Gaussia* luciferase assay kit (New England Biolabs, Inc.) on a Lucy 2 luminometer (Anthos Labtec Instruments). Specific binding values were calculated for the two GpL fusion proteins by subtracting the values obtained for empty vector–transfected cells (nonspecific binding) from the corresponding values verified for the TNFR2 transfectants. To analyze the binding of wild-type mouse TNF and STAR2 to mouse TNFR1, a black high-bond 96-well ELISA plate coated with 0.5 µg/ml protein G was loaded with 1 µg/ml of an Fc fusion protein of the ectodomain of mouse TNFR1. Wells were then incubated with increasing concentrations of GpL–mouse TNF and GpL-STAR2 for 1 h at 37°C, and the well-associated luciferase activity was quantified using the *Gaussia* luciferase assay kit. B_{max} and K_d values were obtained by fitting the binding data by nonlinear regression to a one side–specific binding plot using Prism5 (GraphPad Software).

Analysis of cell viability and ALP activity

Cell viability was assessed using standard crystal violet staining. To measure ALP activity in BMP2-stimulated mouse preosteoblastic C2C12 cells, the cells were cultivated for 48 h in the presence and absence of TNFR1 and TNFR2 agonists in DMEM with 2% FCS. Finally, cells were lysed, and ALP activity was determined using *p*-nitrophenylphosphate conversion and measuring the absorbance at 405 nm.

Animals

BALB/c, C57BL/6, and FVB/N mice were obtained from Charles River. B6.129S7-Tnfrsf1b^{tm1Imx}/J (B6.TNFR2 KO), C57BL/6-Tnfrsf1a^{tm1Imx}/J (B6.TNFR1 KO), B6.129S-Tnfrsf1a^{tm1Imx}Tnfrsf1b^{tm1Imx}/J (B6.TNFR1R2 KO), and B6.129S6-Tnft^{m1Gkl}/J (B6.TNF KO) (all on a C57BL/6 H-2^{b} background) were initially obtained from The Jackson Laboratory. B6(Cg)-Tyr^{c-2J}/J albino C57BL/6 mice were provided by B. Holtmann (Center for Experimental Molecular Medicine at the University Hospital Würzburg, Würzburg, Germany). C57BL/6.Foxp3.Luci.DTR-4 mice expressing enhanced GFP (eGFP), firefly luciferase, and the human DTx receptor under the control of the Foxp3 promoter (Suffner et al., 2010) were provided by G. Hämmerling (German Cancer Research Center, Heidelberg, Germany). C57BL/6.Foxp3.Luci.DTR-4 mice were backcrossed to albino B6 to generate albino B6.Foxp3.Luci.DTR-4 mice, which are superior to black mice in terms of in vivo BLI sensitivity. The genotypes of transgenic mice were routinely checked by flow cytometry of GFP-expressing PBMCs or standard PCR for B6.TNFR2 KO mice. B6.L2G85.CD90.1 mice ubiquitously expressing firefly luciferase were described previously (Beilhack et al., 2005). Female mice were used for experiments between 8 and 12 wk of age. All mice were bred within the specified pathogen-free animal facilities of the Center for Experimental Molecular Medicine at the Würzburg University Hospital or in the Central Laboratory Animal Facility at the University Medical Center of the Johannes Gutenberg University, Mainz. Mice received rodent chow and autoclaved drinking water ad libitum. All animal experiments were approved by local authorities (animal ethics committee of the Regierung von Unterfranken 55.2–2531.01-12/13; animal ethics committee of the Landesuntersuchungsamt Rheinland-Pfalz 177–07/G09-1-004) and complied with German animal protection laws.

Cell culture

A20 yellow fluorescent protein (yfp)/luc mouse B cell lymphoma (H-2^d) cells expressing firefly luciferase and yfp (Edinger et al., 2003) and IM380 mouse B cell lymphoma (H-2^d) cells expressing firefly luciferase and eGFP (Chopra et al., 2013b) were maintained in complete RPMI medium and passaged twice weekly. Both cell lines are syngeneic to BALB/c mice.

Cell isolation from the bone marrow, spleen, lungs, and intestinal tract

Bone marrow cells were isolated from BALB/c, C57BL/6, or FVB/N mice. Femur and tibia bones were flushed with PBS, and the cell suspension was filtered through a 70-µm cell strainer (BD). Spleens were directly filtered through a 70-µm cell strainer into erythrocyte lysis buffer (168 mM NH_4Cl, 10 mM $KHCO_3$, and 0.1 mM EDTA). T cells were enriched from the splenocytes using the Dynal Mouse T cell Negative Isolation kit (Invitrogen) according to the manufacturer's instructions. Negative isolated T cells were stained with anti-CD25 PE-labeled mAb (PC61; BD), and $CD4^+CD25^+$ or $CD4^+CD25^-$ cells were enriched by anti-PE magnetic-activated cell-sorting beads (Miltenyi Biotec). Lung and gut samples were minced with a surgical blade and digested for 45 min at 37°C with 2 mg/ml collagenase D and 0.1 mg/ml DNase I (both from Roche). Tissue pieces were mashed through a 70-µm cell strainer and spun down. The cell pellet was resuspended in erythrocyte lysis buffer.

Isolation of $CD4^+$ T cells from human PBMCs

Human peripheral blood samples were obtained from the Department of Transfusion Medicine at the University Hospital Würzburg, and use of the samples complied with the approval of the University Hospital of Würzburg Ethical Committee. PBMCs were isolated by standard Ficoll gradient centrifugation (Bicoll; Biochrom). $CD4^+$ T cells were enriched using a human $CD4^+$ T cell isolation kit (Miltenyi Biotec).

T cell cultures

Enriched T cells were cultured in 96-well round-bottom plates in complete RPMI medium for 96 h. Primary $CD4^+CD25^-$ T con cells were differentiated in IMDM (5% FCS; Invitrogen) for 72 h using a combination of plate-bound αCD3 mAb (145-2C11; 1–5 µg/ml) and αCD28 mAb (37.51; 1–10 µg/ml; both BD) in the presence of 50 U/ml recombinant human IL-2 (PeproTech), 2–5 ng/ml human TGF-β (PeproTech), 5 µg/ml anti–IFN-γ (R&D Systems), 5 µg/ml anti–IL-4 (R&D Systems), and 5 µg/ml anti–IL-12 (R&D Systems).

Cytometric bead array

Serum and tissue cytokine concentrations were determined using a cytometric bead array kit (BD) according to the manufacturer's protocol. Data were analyzed by FCAP Array software (version 2.0).

Allo-HCT, GvHD, and GvL models

Host mice were injected i.p. with 75 µg (416 pmol) STAR2 in 200 µl PBS on days 14, 12, 10, 7, 5, and 3 with respect to the day of allo-HCT. To study the influence of T reg cell depletion, B6.Foxp3.Luci.DTR-4 mice (untreated or pretreated with STAR2 for 2 wk) were injected i.p. with 15 ng/g bw DTx in 200 µl PBS on days 2 and 1 in respect to the day of transplantation.

Transgenic albino B6.Foxp3.Luci.DTR-4 mice, TNFR2 KO mice, and their wild-type littermates were lethally irradiated at a dose of 9 Gy using an x-ray irradiation system (CP-160; Faxitron X-Ray) and injected with 5×10^6 allogeneic bone marrow cells and 10^6 enriched T cells, both isolated from FVB/N donor mice. BALB/c mice were lethally irradiated with a dose of 8 Gy and injected with 5×10^6 allogeneic bone marrow cells isolated from B6 donor mice and 10^6 enriched T cells from luc^+ B6.L2G85.CD90.1 mice. Donor cells in 100 µl PBS were injected i.v. into the retro-orbital plexus of irradiated host mice.

For GvL experiments, 10^5 A20 yfp/luc cells in 100 µl PBS were injected into the lateral tail vein of host mice after irradiation and the transfer of bone marrow and T cells. For the IM380 model, 10^5 cells were injected into the lateral tail vein of host mice 6 d before allo-HCT.

Mice were treated with antibiotic drinking water (Baytril; Bayer) for 1 wk to prevent infections after myeloablative irradiation. Transplanted mice were assessed for weight loss and clinical scoring for GvHD and leukemia symptoms (Cooke et al., 1996) at indicated time points until the end of the experiment.

In vivo BLI

Mice were anesthetized with i.p. injection of 80 mg/kg bw esketamine hydrochloride (Pfizer) and 16 mg/kg bw xylazine (cp Pharma). Together with anesthetics, mice were injected with 300 mg/kg bw D-luciferin (Biosynth). 10 min later, bioluminescence signals from the anesthetized mice were recorded using an imaging system (IVIS Spectrum; Caliper Life Sciences). Pictures were taken in automatic mode with a maximum exposure time of 5 min per picture and analyzed using Living Image software (version 4.0; Caliper Life Sciences).

Ex vivo imaging, tissue sample preparation, and histopathological evaluation

Mice were injected with D-luciferin and euthanized 10 min later. Internal organs were removed and subjected to ex vivo BLI (Beilhack et al., 2005). Tissue samples were embedded in optimal cutting temperature compound (Tissue Tek; Sakura) or stored in 4% paraformaldehyde in PBS for further standard hematoxylin/eosin histopathological analysis and scored for the following endpoints (scores of 0–4 depending on severity): crypt apoptosis, inflammation, and crypt loss in the small and large bowel; bile duct injury, vascular injury, hepatocellular damage, and portal inflammation in the liver; and (with scores of 0–3 depending on severity) apoptosis, ballooning of the basal layer, and inflammation

in the skin. Samples from the spleen and small and large bowel were stored in PBS on ice for immune cell isolation and flow cytometry.

Flow cytometry

Cells were blocked with normal rat serum (1:20 in PBS) and stained with the appropriate antibodies (Table S1) at 4°C for 30 min. Cells were stained using fixable live/dead cell stain kits (Invitrogen or BioLegend) and antibodies for surface antigens and then further processed using a Mouse Regulatory T Cell Staining kit (no. 2; eBioscience) according to the manufacturer's protocol. All experiments were analyzed on a cell analyzer (FACS Canto II; BD), and the sample data were recorded using FACSDiva software (BD) and analyzed using FlowJo software (Tree Star).

Immunofluorescence microscopy

Cryo-embedded tissues were cut into 3-µm-thick sections on a cryostat (CM1900; Leica Biosystems) and mounted onto frosted slides. The slides were air dried, fixed with acetone at room temperature, washed, and blocked with 2% FCS in PBS for 15 min. When biotin-conjugated antibodies were used, additional blocking was performed using an avidin/biotin blocking kit (Vector Laboratories). The slides were then incubated with the appropriate antibodies (1:100; Table S1) for 1 h at room temperature, counterstained with DAPI, and mounted with mounting medium (Vector Laboratories). Images were obtained with a fluorescence microscope (Imager.Z1m; ZEISS) at room temperature and evaluated using AxioVision software (ZEISS).

For confocal laser-scanning microscopy, paraffin-embedded biopsies of the large bowel from allogeneic-transplanted human patients were sectioned, deparaffinized, and pretreated with cell stabilizing buffer, pH 6.0. Sections were incubated with primary antibodies (rat anti-Foxp3, 1:100; and rabbit anti-TNFR2, 1:250; Table S1) for 1 h followed by secondary antibodies (1:400) for 1 h. Sections were analyzed using a confocal laser-scanning microscope (TCS SP2; Leica Biosystems) and confocal software (Leica Biosystems).

Syngeneic HTC/allo-HCT and mCMV infection

Female BALB/c mice were pretreated i.p. with 75 µg (416 pM) STAR2 in PBS on days 14, 12, 10, 7, 5, and 3 with respect to the day of HCT or were treated with PBS for control. HCT and mCMV infections were performed with both groups as described previously (Podlech et al., 2000). In brief, HCT recipients were immunocompromised by myeloablative total-body γ irradiation with a single dose of 6.5 Gy. HCT was performed 6 h later by infusion of 5×10^6 bone marrow cells derived from either BALB/c (syngeneic setting) or BALB/c-H-2^{dm2} (allogeneic setting; these mice lack the MHC class I L^d molecule because of a genetic deletion; Rubocki et al., 1986) into the tail vein of the recipients. Intraplantar infection of the recipients with 10^5 PFU of wild-type virus mCMV-WT.Smith (strain Smith ATCC VR-1399) was performed 2 h after HCT.

Quantitation of mCMV infection in host tissues

Infectious virus at 18 d (allogeneic setting) or 4 wk (syngeneic setting) after HCT and infection was quantitated in organ homogenates by the virus plaque (PFU) assay on mouse embryo fibroblast monolayers (Podlech et al., 2000). mCMV infection and T cell infiltration of the liver was assessed by two-color immunohistochemistry with red staining of the intranuclear viral protein IE1-pp89/76 (mAb clone Croma 101) and black membrane staining of CD3ε (mAb clone CD3-12)-expressing lymphocytes (Podlech et al., 2000).

Preparation and phenotypic analysis of lung leukocytes

Interstitial pulmonary leukocytes were isolated as previously described (Podlech et al., 2000). In brief, lungs were perfused via the right ventricle with perfusion solution (PBS + 10 U/ml Heparin) and were excised. Tracheae, bronchi, and pulmonary lymph nodes were carefully removed, the lobe of the left lung was stored for the virus plaque assay (Podlech et al., 2000), and the remaining four lung lobes were minced with scissors. Digestion of pooled lobes from three to four lungs was performed in 15 ml DMEM + 0.4 U/ml collagenase A (Roche) + 33 U/ml DNase I (Sigma-Aldrich) for 1 h at 37°C with constant stirring. Tissue clumps were resolved by straining the digested tissue through a steel mesh. Cells were washed and passed through a 100-µm nylon mesh, and mononuclear leukocytes were enriched by density gradient centrifugation.

For cytofluorometric analysis, leukocytes isolated from the lungs of three to four mice per group were labeled with an MHC-peptide multimer (dextramer H-2Dd-m164[AGPPRYSRI] PE conjugated; 10 µl per 10^6 cells; catalog no. JB3533-PE; Immudex) to detect m164 epitope–specific TCRs together with directly fluorochrome-conjugated mAbs. Analysis was performed with FC500 and CXP software (version 2.2; Beckman Coulter).

Statistical analysis

All data are reported as mean ± SEM and represent combined data from at least two independent experiments unless noted otherwise. Figures were prepared using Prism 5 (GraphPad Software) and Photoshop 7 (Adobe). Different groups were compared by two-tailed unpaired Student's *t* tests using InStat 3 (GraphPad Software) unless noted otherwise. Significance was set at $P \leq 0.05$.

Online supplemental material

Table S1 shows the antibodies used in this study. Online supplemental material is available at http://www.jem.org/cgi/content/full/jem.20151563/DC1.

ACKNOWLEDGMENTS

We acknowledge Christian Linden for his help with the cell-sorting experiments.

This work was supported by the Interdisziplinäre Zentrum für Klinische Forschung der Universität Würzburg (B-149 and B-233), the IFF-I program of the Johannes Gutenberg University, Mainz, the Deutsche José Carreras Leukämie-Stiftung e.V. (R/06/17 and R/10/15), the Deutsche Forschungsgemeinschaft (SFBTR 124 A3, SFBTR 52 Z2, Wa 1025/18-1, KFO183 TP8, KFO 216 TP8/Z1, and Ma 760/19-1), and the Else-Kröner-Fresenius-Stiftung (2010_Kolleg.52).

The authors declare no competing financial interests.

Submitted: 29 September 2015

Accepted: 24 June 2016

REFERENCES

Anderson, B.E., J.M. McNiff, C. Matte, I. Athanasiadis, W.D. Shlomchik, and M.J. Shlomchik. 2004. Recipient $CD4^+$ T cells that survive irradiation regulate chronic graft-versus-host disease. *Blood*. 104:1565–1573. http://dx.doi.org/10.1182/blood-2004-01-0328

Ban, L., W. Kuhtreiber, J. Butterworth, Y. Okubo, É.S. Vanamee, and D.L. Faustman. 2015. Strategic internal covalent cross-linking of TNF produces a stable TNF trimer with improved TNFR2 signaling. *Mol. Cell. Ther.* 3:7. http://dx.doi.org/10.1186/s40591-015-0044-4

Beilhack, A., S. Schulz, J. Baker, G.F. Beilhack, C.B. Wieland, E.I. Herman, E.M. Baker, Y.A. Cao, C.H. Contag, and R.S. Negrin. 2005. In vivo analyses of early events in acute graft-versus-host disease reveal sequential infiltration of T-cell subsets. *Blood*. 106:1113–1122. http://dx.doi.org/10.1182/blood-2005-02-0509

Beilhack, A., S. Schulz, J. Baker, G.F. Beilhack, R. Nishimura, E.M. Baker, G. Landan, E.I. Herman, E.C. Butcher, C.H. Contag, and R.S. Negrin. 2008. Prevention of acute graft-versus-host disease by blocking T-cell entry to secondary lymphoid organs. *Blood*. 111:2919–2928. http://dx.doi.org/10.1182/blood-2007-09-112789

Brunstein, C.G., J.S. Miller, Q. Cao, D.H. McKenna, K.L. Hippen, J. Curtsinger, T. Defor, B.L. Levine, C.H. June, P. Rubinstein, et al. 2011. Infusion of ex vivo expanded T regulatory cells in adults transplanted with umbilical cord blood: safety profile and detection kinetics. *Blood*. 117:1061–1070. http://dx.doi.org/10.1182/blood-2010-07-293795

Casares, N., F. Rudilla, L. Arribillaga, D. Llopiz, J.I. Riezu-Boj, T. Lozano, J. López-Sagaseta, L. Guembe, P. Sarobe, J. Prieto, et al. 2010. A peptide inhibitor of FOXP3 impairs regulatory T cell activity and improves vaccine efficacy in mice. *J. Immunol.* 185:5150–5159. http://dx.doi.org/10.4049/jimmunol.1001114

Chen, X., M. Bäumel, D.N. Männel, O.M. Howard, and J.J. Oppenheim. 2007. Interaction of TNF with TNF receptor type 2 promotes expansion and function of mouse $CD4^+CD25^+$ T regulatory cells. *J. Immunol.* 179:154–161. http://dx.doi.org/10.4049/jimmunol.179.1.154

Chen, X., J.J. Subleski, H. Kopf, O.M. Howard, D.N. Männel, and J.J. Oppenheim. 2008. Cutting edge: expression of TNFR2 defines a maximally suppressive subset of mouse $CD4^+CD25^+FoxP3^+$ T regulatory cells: applicability to tumor-infiltrating T regulatory cells. *J. Immunol.* 180:6467–6471. http://dx.doi.org/10.4049/jimmunol.180.10.6467

Chen, X., R. Hamano, J.J. Subleski, A.A. Hurwitz, O.M. Howard, and J.J. Oppenheim. 2010b. Expression of costimulatory TNFR2 induces resistance of $CD4^+FoxP3^-$ conventional T cells to suppression by $CD4^+FoxP3^+$ regulatory T cells. *J. Immunol.* 185:174–182. http://dx.doi.org/10.4049/jimmunol.0903548

Chen, X., J.J. Subleski, R. Hamano, O.M. Howard, R.H. Wiltrout, and J.J. Oppenheim. 2010a. Co-expression of TNFR2 and CD25 identifies more of the functional $CD4^+FOXP3^+$ regulatory T cells in human peripheral blood. *Eur. J. Immunol.* 40:1099–1106. http://dx.doi.org/10.1002/eji.200940022

Chen, X., X. Wu, Q. Zhou, O.M. Howard, M.G. Netea, and J.J. Oppenheim. 2013. TNFR2 is critical for the stabilization of the $CD4^+Foxp3^+$ regulatory T. cell phenotype in the inflammatory environment. *J. Immunol.* 190:1076–1084. http://dx.doi.org/10.4049/jimmunol.1202659

Chopra, M., S. Kraus, S. Schwinn, M. Ritz, K. Mattenheimer, A. Mottok, A. Rosenwald, H. Einsele, and A. Beilhack. 2013b. Non-invasive bioluminescence imaging to monitor the immunological control of a plasmablastic lymphoma-like B cell neoplasia after hematopoietic cell transplantation. *PLoS One.* 8:e81320. http://dx.doi.org/10.1371/journal.pone.0081320

Chopra, M., S.S. Riedel, M. Biehl, S. Krieger, V. von Krosigk, C.A. Bäuerlein, C. Brede, A.L. Jordan Garrote, S. Kraus, V. Schäfer, et al. 2013a. Tumor necrosis factor receptor 2-dependent homeostasis of regulatory T cells as a player in TNF-induced experimental metastasis. *Carcinogenesis.* 34:1296–1303. http://dx.doi.org/10.1093/carcin/bgt038

Chopra, M., A. Brandl, D. Siegmund, A. Mottok, V. Schäfer, M. Biehl, S. Kraus, C.A. Bäuerlein, M. Ritz, K. Mattenheimer, et al. 2015. Blocking TWEAK-Fn14 interaction inhibits hematopoietic stem cell transplantation-induced intestinal cell death and reduces GVHD. *Blood*. 126:437–444. http://dx.doi.org/10.1182/blood-2015-01-620583

Coghill, J.M., M.J. Carlson, A. Panoskaltsis-Mortari, M.L. West, J.E. Burgents, B.R. Blazar, and J.S. Serody. 2010. Separation of graft-versus-host disease from graft-versus-leukemia responses by targeting CC-chemokine receptor 7 on donor T cells. *Blood*. 115:4914–4922. http://dx.doi.org/10.1182/blood-2009-08-239848

Cooke, K.R., L. Kobzik, T.R. Martin, J. Brewer, J. Delmonte Jr., J.M. Crawford, and J.L. Ferrara. 1996. An experimental model of idiopathic pneumonia syndrome after bone marrow transplantation: I. The roles of minor H antigens and endotoxin. *Blood*. 88:3230–3239.

Di Ianni, M., F. Falzetti, A. Carotti, A. Terenzi, F. Castellino, E. Bonifacio, B. Del Papa, T. Zei, R.I. Ostini, D. Cecchini, et al. 2011. Tregs prevent GVHD and promote immune reconstitution in HLA-haploidentical transplantation. *Blood*. 117:3921–3928. http://dx.doi.org/10.1182/blood-2010-10-311894

Edinger, M., and P. Hoffmann. 2011. Regulatory T cells in stem cell transplantation: strategies and first clinical experiences. *Curr. Opin. Immunol.* 23:679–684. http://dx.doi.org/10.1016/j.coi.2011.06.006

Edinger, M., P. Hoffmann, J. Ermann, K. Drago, C.G. Fathman, S. Strober, and R.S. Negrin. 2003. $CD4^+CD25^+$ regulatory T cells preserve graft-versus-tumor activity while inhibiting graft-versus-host disease after bone marrow transplantation. *Nat. Med.* 9:1144–1150. http://dx.doi.org/10.1038/nm915

Ehrenstein, M.R., J.G. Evans, A. Singh, S. Moore, G. Warnes, D.A. Isenberg, and C. Mauri. 2004. Compromised function of regulatory T cells in rheumatoid arthritis and reversal by anti-TNFalpha therapy. *J. Exp. Med.* 200:277–285. http://dx.doi.org/10.1084/jem.20040165

Feldmann, M., and R.N. Maini. 2003. TNF defined as a therapeutic target for rheumatoid arthritis and other autoimmune diseases. *Nat. Med.* 9:1245–1250. http://dx.doi.org/10.1038/nm939

Grell, M., E. Douni, H. Wajant, M. Löhden, M. Clauss, B. Maxeiner, S. Georgopoulos, W. Lesslauer, G. Kollias, K. Pfizenmaier, and P. Scheurich. 1995. The transmembrane form of tumor necrosis factor is the prime activating ligand of the 80 kDa tumor necrosis factor receptor. *Cell*. 83:793–802. http://dx.doi.org/10.1016/0092-8674(95)90192-2

Grinberg-Bleyer, Y., D. Saadoun, A. Baeyens, F. Billiard, J.D. Goldstein, S. Grégoire, G.H. Martin, R. Elhage, N. Derian, W. Carpentier, et al. 2010. Pathogenic T cells have a paradoxical protective effect in murine autoimmune diabetes by boosting Tregs. *J. Clin. Invest.* 120:4558–4568. http://dx.doi.org/10.1172/JCI42945

Hebart, H., and H. Einsele. 2004. Clinical aspects of CMV infection after stem cell transplantation. *Hum. Immunol.* 65:432–436. http://dx.doi.org/10.1016/j.humimm.2004.02.022

Hoffmann, P., J. Ermann, M. Edinger, C.G. Fathman, and S. Strober. 2002. Donor-type $CD4^+CD25^+$ regulatory T cells suppress lethal acute graft-versus-host disease after allogeneic bone marrow transplantation. *J. Exp. Med.* 196:389–399. http://dx.doi.org/10.1084/jem.20020399

Housley, W.J., C.O. Adams, F.C. Nichols, L. Puddington, E.G. Lingenheld, L. Zhu, T.V. Rajan, and R.B. Clark. 2011. Natural but not inducible regulatory T cells require TNF-α signaling for in vivo function. *J. Immunol.* 186:6779–6787. http://dx.doi.org/10.4049/jimmunol.1003868

Jones, S.C., G.F. Murphy, and R. Korngold. 2003. Post-hematopoietic cell transplantation control of graft-versus-host disease by donor CD425 T cells to allow an effective graft-versus-leukemia response. *Biol. Blood Marrow Transplant.* 9:243–256. http://dx.doi.org/10.1053/bbmt.2003.50027

Kim, Y.M., T. Sachs, W. Asavaroengchai, R. Bronson, and M. Sykes. 2003. Graft-versus-host disease can be separated from graft-versus-lymphoma effects by control of lymphocyte trafficking with FTY720. *J. Clin. Invest.* 111:659–669. http://dx.doi.org/10.1172/JCI200316950

Klages, K., C.T. Mayer, K. Lahl, C. Loddenkemper, M.W. Teng, S.F. Ngiow, M.J. Smyth, A. Hamann, J. Huehn, and T. Sparwasser. 2010. Selective depletion of $Foxp3^+$ regulatory T cells improves effective therapeutic vaccination against established melanoma. *Cancer Res.* 70:7788–7799. http://dx.doi.org/10.1158/0008-5472.CAN-10-1736

Ko, J.M., A.B. Gottlieb, and J.F. Kerbleski. 2009. Induction and exacerbation of psoriasis with TNF-blockade therapy: a review and analysis of 127 cases. *J. Dermatolog. Treat.* 20:100–108. http://dx.doi.org/10.1080/09546630802441234

Komatsu, N., and S. Hori. 2007. Full restoration of peripheral $Foxp3^+$ regulatory T cell pool by radioresistant host cells in *scurfy* bone marrow chimeras. *Proc. Natl. Acad. Sci. USA.* 104:8959–8964. http://dx.doi.org/10.1073/pnas.0702004104

Levine, J.E. 2011. Implications of TNF-α in the pathogenesis and management of GVHD. *Int. J. Hematol.* 93:571–577. http://dx.doi.org/10.1007/s12185-011-0803-1

Lewis, M., L.A. Tartaglia, A. Lee, G.L. Bennett, G.C. Rice, G.H. Wong, E.Y. Chen, and D.V. Goeddel. 1991. Cloning and expression of cDNAs for two distinct murine tumor necrosis factor receptors demonstrate one receptor is species specific. *Proc. Natl. Acad. Sci. USA.* 88:2830–2834. http://dx.doi.org/10.1073/pnas.88.7.2830

Li, H.W., and M. Sykes. 2012. Emerging concepts in haematopoietic cell transplantation. *Nat. Rev. Immunol.* 12:403–416. http://dx.doi.org/10.1038/nri3226

Lin, Y.L., C.C. Shieh, and J.Y. Wang. 2008. The functional insufficiency of human $CD4^+CD25^{high}$ T-regulatory cells in allergic asthma is subjected to TNF-α modulation. *Allergy.* 63:67–74. http://dx.doi.org/10.1111/j.1398-9995.2007.01526.x

Loetscher, H., D. Stueber, D. Banner, F. Mackay, and W. Lesslauer. 1993. Human tumor necrosis factor α (TNF α) mutants with exclusive specificity for the 55-kDa or 75-kDa TNF receptors. *J. Biol. Chem.* 268:26350–26357.

Marr, K.A., R.A. Carter, M. Boeckh, P. Martin, and L. Corey. 2002. Invasive aspergillosis in allogeneic stem cell transplant recipients: changes in epidemiology and risk factors. *Blood.* 100:4358–4366. http://dx.doi.org/10.1182/blood-2002-05-1496

Martelli, M.F., M. Di Ianni, L. Ruggeri, F. Falzetti, A. Carotti, A. Terenzi, A. Pierini, M.S. Massei, L. Amico, E. Urbani, et al. 2014. HLA-haploidentical transplantation with regulatory and conventional T-cell adoptive immunotherapy prevents acute leukemia relapse. *Blood.* 124:638–644. http://dx.doi.org/10.1182/blood-2014-03-564401

Miller, P.G., M.B. Bonn, and S.C. McKarns. 2015. Transmembrane TNF-TNFR2 impairs Th17 differentiation by promoting IL2 expression. *J. Immunol.* 195:2633–2647. http://dx.doi.org/10.4049/jimmunol.1500286

Nadkarni, S., C. Mauri, and M.R. Ehrenstein. 2007. Anti-TNF-α therapy induces a distinct regulatory T cell population in patients with rheumatoid arthritis via TGF-β. *J. Exp. Med.* 204:33–39. http://dx.doi.org/10.1084/jem.20061531

Nagar, M., J. Jacob-Hirsch, H. Vernitsky, Y. Berkun, S. Ben-Horin, N. Amariglio, I. Bank, Y. Kloog, G. Rechavi, and I. Goldstein. 2010. TNF activates a NF-κB-regulated cellular program in human $CD45RA^-$ regulatory T cells that modulates their suppressive function. *J. Immunol.* 184:3570–3581. http://dx.doi.org/10.4049/jimmunol.0902070

Nguyen, V.H., R. Zeiser, D.L. Dasilva, D.S. Chang, A. Beilhack, C.H. Contag, and R.S. Negrin. 2007. In vivo dynamics of regulatory T-cell trafficking and survival predict effective strategies to control graft-versus-host disease following allogeneic transplantation. *Blood.* 109:2649–2656. http://dx.doi.org/10.1182/blood-2006-08-044529

Nie, H., Y. Zheng, R. Li, T.B. Guo, D. He, L. Fang, X. Liu, L. Xiao, X. Chen, B. Wan, et al. 2013. Phosphorylation of FOXP3 controls regulatory T cell function and is inhibited by TNF-α in rheumatoid arthritis. *Nat. Med.* 19:322–328. http://dx.doi.org/10.1038/nm.3085

Okubo, Y., T. Mera, L. Wang, and D.L. Faustman. 2013. Homogeneous expansion of human T-regulatory cells via tumor necrosis factor receptor 2. *Sci. Rep.* 3:3153. http://dx.doi.org/10.1038/srep03153

Pierini, A., L. Colonna, M. Alvarez, D. Schneidawind, H. Nishikii, J. Baker, Y. Pan, M. Florek, B.S. Kim, and R.S. Negrin. 2015. Donor requirements for regulatory T cell suppression of murine graft-versus-host disease. *J. Immunol.* 195:347–355. http://dx.doi.org/10.4049/jimmunol.1402861

Podlech, J., R. Holtappels, M.F. Pahl-Seibert, H.P. Steffens, and M.J. Reddehase. 2000. Murine model of interstitial cytomegalovirus pneumonia in syngeneic bone marrow transplantation: persistence of protective pulmonary CD8-T-cell infiltrates after clearance of acute infection. *J. Virol.* 74:7496–7507. http://dx.doi.org/10.1128/JVI.74.16.7496-7507.2000

Podlech, J., R. Holtappels, N.K.A. Grzimek, and M.J. Reddehase. 2002. Animal models: murine cytomegalovirus. *In* Immunology of Infection. S.H.E. Kaufmann and D. Kabelitz, editors. Academic Press, San Diego. 493–525. http://dx.doi.org/10.1016/S0580-9517(02)32103-2

Ramos-Casals, M., P. Brito-Zerón, M.J. Soto, M.J. Cuadrado, and M.A. Khamashta. 2008. Autoimmune diseases induced by TNF-targeted therapies. *Best Pract. Res. Clin. Rheumatol.* 22:847–861. http://dx.doi.org/10.1016/j.berh.2008.09.008

Rauert, H., A. Wicovsky, N. Müller, D. Siegmund, V. Spindler, J. Waschke, C. Kneitz, and H. Wajant. 2010. Membrane tumor necrosis factor (TNF) induces p100 processing via TNF receptor-2 (TNFR2). *J. Biol. Chem.* 285:7394–7404. http://dx.doi.org/10.1074/jbc.M109.037341

Robinson, W.H., M.C. Genovese, and L.W. Moreland. 2001. Demyelinating and neurologic events reported in association with tumor necrosis factor α antagonism: by what mechanisms could tumor necrosis factor α antagonists improve rheumatoid arthritis but exacerbate multiple sclerosis? *Arthritis Rheum.* 44:1977–1983. http://dx.doi.org/10.1002/1529-0131(200109)44:9<1977::AID-ART345>3.0.CO;2-6

Römer, P.S., S. Berr, E. Avota, S.Y. Na, M. Battaglia, I. ten Berge, H. Einsele, and T. Hünig. 2011. Preculture of PBMCs at high cell density increases sensitivity of T-cell responses, revealing cytokine release by CD28 superagonist TGN1412. *Blood.* 118:6772–6782. http://dx.doi.org/10.1182/blood-2010-12-319780

Rubocki, R.J., T.H. Hansen, and D.R. Lee. 1986. Molecular studies of murine mutant BALB/c-$H\text{-}2^{dm2}$ define a deletion of several class I genes including the entire H-2Ld gene. *Proc. Natl. Acad. Sci. USA.* 83:9606–9610. http://dx.doi.org/10.1073/pnas.83.24.9606

Schneidawind, D., A. Pierini, and R.S. Negrin. 2013. Regulatory T cells and natural killer T cells for modulation of GVHD following allogeneic hematopoietic cell transplantation. *Blood.* 122:3116–3121. http://dx.doi.org/10.1182/blood-2013-08-453126

Schneidawind, D., A. Pierini, M. Alvarez, Y. Pan, J. Baker, C. Buechele, R.H. Luong, E.H. Meyer, and R.S. Negrin. 2014. CD4+ invariant natural killer T cells protect from murine GVHD lethality through expansion of donor CD4+CD25+FoxP3+ regulatory T cells. *Blood*. 124:3320–3328. http://dx.doi.org/10.1182/blood-2014-05-576017

Schneider, P., N. Holler, J.L. Bodmer, M. Hahne, K. Frei, A. Fontana, and J. Tschopp. 1998. Conversion of membrane-bound Fas(CD95) ligand to its soluble form is associated with downregulation of its proapoptotic activity and loss of liver toxicity. *J. Exp. Med.* 187:1205–1213. http://dx.doi.org/10.1084/jem.187.8.1205

Suffner, J., K. Hochweller, M.C. Kühnle, X. Li, R.A. Kroczek, N. Garbi, and G.J. Hämmerling. 2010. Dendritic cells support homeostatic expansion of Foxp3$^+$ regulatory T cells in Foxp3.LuciDTR mice. *J. Immunol.* 184:1810–1820. http://dx.doi.org/10.4049/jimmunol.0902420

Trenado, A., F. Charlotte, S. Fisson, M. Yagello, D. Klatzmann, B.L. Salomon, and J.L. Cohen. 2003. Recipient-type specific CD4$^+$CD25$^+$ regulatory T cells favor immune reconstitution and control graft-versus-host disease while maintaining graft-versus-leukemia. *J. Clin. Invest.* 112:1688–1696. http://dx.doi.org/10.1172/JCI17702

Tsakiri, N., D. Papadopoulos, M.C. Denis, D.D. Mitsikostas, and G. Kollias. 2012. TNFR2 on non-haematopoietic cells is required for Foxp3$^+$ Treg-cell function and disease suppression in EAE. *Eur. J. Immunol.* 42:403–412. http://dx.doi.org/10.1002/eji.201141659

Valencia, X., G. Stephens, R. Goldbach-Mansky, M. Wilson, E.M. Shevach, and P.E. Lipsky. 2006. TNF downmodulates the function of human CD4$^+$CD25^{hi} T-regulatory cells. *Blood.* 108:253–261. http://dx.doi.org/10.1182/blood-2005-11-4567

Veerapathran, A., J. Pidala, F. Beato, B. Betts, J. Kim, J.G. Turner, M.K. Hellerstein, X.Z. Yu, W. Janssen, and C. Anasetti. 2013. Human regulatory T cells against minor histocompatibility antigens: ex vivo expansion for prevention of graft-versus-host disease. *Blood.* 122:2251–2261. http://dx.doi.org/10.1182/blood-2013-03-492397

Welniak, L.A., B.R. Blazar, and W.J. Murphy. 2007. Immunobiology of allogeneic hematopoietic stem cell transplantation. *Annu. Rev. Immunol.* 25:139–170. http://dx.doi.org/10.1146/annurev.immunol.25.022106.141606

Zhang, Q., F. Cui, L. Fang, J. Hong, B. Zheng, and J.Z. Zhang. 2013. TNF-α impairs differentiation and function of TGF-β-induced Treg cells in autoimmune diseases through Akt and Smad3 signaling pathway. *J. Mol. Cell Biol.* 5:85–98. http://dx.doi.org/10.1093/jmcb/mjs063